PROSTHETICS

Augmenting rehabilitation robotics with spinal cord neuromodulation: A proof of concept

Nicolas Hankov[1,2,3]†, Miroslav Caban[1,4,5]†, Robin Demesmaeker[1,2,3], Margaux Roulet[1,2,3], Salif Komi[1,2,3], Michele Xiloyannis[6,7], Anne Gehrig[8], Camille Varescon[1,2,3], Martina Rebeka Spiess[9,10], Serena Maggioni[7,9], Chiara Basla[6,7], Gleb Koginov[6,11], Florian Haufe[6,7], Marina D'Ercole[5], Cathal Harte[1,2,3], Sergio D. Hernandez-Charpak[1,2,3], Aurelie Paley[2,3], Manon Tschopp[2,3], Natacha Herrmann[2,3], Nadine Intering[1,2,3], Edeny Baaklini[1,2,3], Francesco Acquati[1,5], Charlotte Jacquet[5], Anne Watrin[5], Jimmy Ravier[1,2,3], Frédéric Merlos[1,2,3], Grégoire Eberlé[2], Katrien Van den Keybus[2], Hendrik Lambert[5], Henri Lorach[1,2,3], Rik Buschman[12], Nicholas Buse[12], Timothy Denison[13], Dino De Bon[8], Jaime E. Duarte[11], Robert Riener[6,7], Auke Ijspeert[4], Fabien Wagner[1,2,3,14], Sebastian Tobler[15,16], Léonie Asboth[1,2,3], Joachim von Zitzewitz[5]*‡, Jocelyne Bloch[1,2,3,17]*‡, Grégoire Courtine[1,2,3,17]*‡

Rehabilitation robotics aims to promote activity-dependent reorganization of the nervous system. However, people with paralysis cannot generate sufficient activity during robot-assisted rehabilitation and, consequently, do not benefit from these therapies. Here, we developed an implantable spinal cord neuroprosthesis operating in a closed loop to promote robust activity during walking and cycling assisted by robotic devices. This neuroprosthesis is device agnostic and designed for seamless implementation by nonexpert users. Preliminary evaluations in participants with paralysis showed that the neuroprosthesis enabled well-organized patterns of muscle activity during robot-assisted walking and cycling. A proof-of-concept study suggested that robot-assisted rehabilitation augmented by the neuroprosthesis promoted sustained neurological improvements. Moreover, the neuroprosthesis augmented recreational walking and cycling activities outdoors. Future clinical trials will have to confirm these findings in a broader population.

INTRODUCTION

Gait rehabilitation is the only common therapy to augment recovery of ambulation from neurological disorders, including spinal cord injury (SCI) (*1*–*3*). Mounting evidence indicates that gait rehabilitation promotes activity-dependent reorganization of the nervous system, which augments functional recovery (*1*, *4*, *5*). This mechanism of action defines the principles for effective therapies: the robust, coordinated, and repeated activation of the neuromuscular system is critical to promote the activity-dependent reorganization of the nervous system that maximizes neurological recovery (*4*, *6*, *7*). This knowledge has been translated into the design of robotic systems that aim to leverage sensory information patterns to activate the neuromuscular system (*8*–*14*). However, this strategy based on mechanically driven motion of the limbs to augment activity remains insufficient to promote robust activation of the neuromuscular system, especially in patients with paralysis (*15*).

This limitation triggered the development of complementary neuroprosthetic strategies that aim to synchronize the activation of the neuromuscular system with robotic systems during gait rehabilitation (*1*, *7*). The main strategy already integrated in clinical practices involves functional electrical stimulation (FES) of muscles (*16*–*18*). However, this methodology presents several limitations (*19*, *20*), such as the impractical placement of electrodes and rapid exhaustion of muscles.

Epidural electrical stimulation (EES) of the spinal cord is an emerging, fully implanted neuroprosthetic solution to promote robust, coordinated, and repeated activation of the neuromuscular system during gait rehabilitation (*5*, *21*–*23*). EES targets motor neurons through the recruitment of large-diameter afferent fibers where they bend to enter the spinal cord through the dorsal root entry zones (*4*, *24*–*28*). Because motor neurons innervating lower limb muscles are distributed along the rostrocaudal extent of the lumbosacral spinal cord, targeting individual dorsal root entry zones enables the recruitment of specific motor neuron ensembles. In turn, the recruitment of individual dorsal root entry zones with a temporal pattern that reproduces the natural activation of motor neurons has restored standing, walking, cycling, and swimming in people with complete paralysis due to SCI (*29*). We refer to this strategy as activity-dependent biomimetic EES.

[1]NeuroX Institute and Brain Mind Institute, School of Life Sciences, Swiss Federal Institute of Technology (EPFL), Lausanne, Switzerland. [2]Department of Clinical Neuroscience, Lausanne University Hospital (CHUV) and University of Lausanne (UNIL), Lausanne, Switzerland. [3]Defitech Center for Interventional Neurotherapies (NeuroRestore), EPFL/CHUV/UNIL, Lausanne, Switzerland. [4]Biorobotics Laboratory, École Polytechnique Fédérale de Lausanne (EPFL), Lausanne, Switzerland. [5]ONWARD Medical, Lausanne, Switzerland. [6]Sensory-Motor Systems Lab, Department of Health Sciences and Technology, Institute of Robotics and Intelligent Systems, ETH Zurich, Zurich, Switzerland. [7]Spinal Cord Injury Center, University Hospital Balgrist, University of Zurich, Zurich, Switzerland. [8]VAMED Management and Service Switzerland AG, Zurich, Switzerland. [9]Hocoma AG, Volketswil, Switzerland. [10]ZHAW, Zurich University of Applied Sciences, School of Health Sciences, Institute of Occupational Therapy, Zurich, Switzerland. [11]Myoswiss AG, Zurich, Switzerland. [12]Medtronic, Minneapolis, MN, USA. [13]Oxford University, Oxford, UK. [14]Institut des Maladies Neurodégénératives (CNRS UMR 5293), Université de Bordeaux, Bordeaux, France. [15]Bern University of Applied Science, SCI Mobility Lab, University of Bern, Bienne, Switzerland. [16]GBY (Go-by-Yourself) SA, Vuisternens-en-Ogoz, Switzerland. [17]Department of Neurosurgery, Lausanne University Hospital (CHUV) and University of Lausanne (UNIL), Lausanne, Switzerland.
*Corresponding author. Email: gregoire.courtine@epfl.ch (G.C.); jocelyne.bloch@chuv.ch (J.B.); joachim.vonzitzewitz@onwd.com (J.V.Z.)
†These authors contributed equally to this work.
‡These authors contributed equally to this work.

These results open the intriguing possibility to integrate EES technologies with robotic systems to maximize the activation of the neuromuscular system during gait rehabilitation. Conversely, EES technologies are not sufficient to support walking in the early stage of the injury or when the injury is severe. Therefore, EES technologies and rehabilitation robotics may promote complementary support for people with SCI. However, this integration requires the delivery of precisely timed EES patterns that match the requirements of widely different robotic systems and environments. This rigorous synchronization is contingent on a flexible technological framework operating in a closed loop that precisely interfaces activity-specific biomimetic EES programs with the various robotic devices commonly used across the continuum of care (*30*).

Here, we developed a technological framework to interface biomimetic EES with robotic devices. Our preliminary evaluations in five participants with SCI showed that biomimetic EES promotes robust activation of the neuromuscular system during robot-assisted walking and cycling. We also report that robotic systems enabled people with severe paralysis to walk when EES alone was insufficient to support independent walking. In turn, a proof-of-concept study suggested that robotically assisted rehabilitation augmented by biomimetic EES may promote the recovery of volitional movements that persist when EES is turned off. Last, we illustrate the potential synergy between biomimetic EES and robotic devices to augment recreational activities outdoors (Movie 1).

RESULTS

Integration of biomimetic EES with robotics

We aimed to deliver biomimetic EES in combination with robotic and/or assistive devices that are commonly used to support rehabilitation across the entire span of functional ambulatory categories (FACs) (*30*). Biomimetic EES requires the delivery of spatially selective EES waveforms that each target specific groups of muscles. Consequently, multiple EES waveforms must be turned on and off with a precise timing that matches the expected activation of the targeted muscles during each phase of robot-assisted movements. This synchronization requires closed-loop control of EES parameters through wireless links that remain within latencies compatible with the timing of muscle activation underlying these movements. This synchronization is contingent on sensor technologies that can detect the phase of the movement and motor intentions with high accuracy and low latency while ensuring the safety of the patient. The overall system is not only expected to be mobile, lightweight, and highly reliable but also must meet the requirements for implanted medical technologies. Last, an ideal feature of this system is the possibility to be implemented by nonexpert users across any approved robotic device without alteration of the device. We aimed to address this ensemble of challenges with the following hardware and software components:

1) Paddle lead. To target the ensemble of dorsal roots involved in the control of leg muscles, we used two types of paddle leads, each integrating 16 electrodes (Fig. 1A). The neurosurgical positioning of the lead was optimized on the basis of personalized computational models of the spine and intraoperative electrophysiology (Fig. 1A).

2) Implantable pulse generator. The paddle lead was connected to the *ACTIVA RC* implantable pulse generator (IPG), which was inserted in the abdomen. We engineered wireless communication modules (*29*, *31*) that enabled closed-loop control over the parameters of EES (Fig. 1A).

3) Neurostimulation platform. Real-time control of EES requires a medical-grade software application that enables wireless updates of EES parameters on the basis of external signals. For this purpose, we developed the C# app that runs on a tablet. The software includes a stimulation scheduler wherein personalized EES waveforms can be injected to program biomimetic EES for each user and activity (Fig. 1A).

4) Control algorithms. We developed an algorithmic framework implemented within the app that supports the flexible configuration of device-specific EES programs, termed EES^{DEVICE}. The algorithm provides the user with the possibility to select the relevant sensing technologies to control EES^{DEVICE} in a closed loop (Fig. 1, B to D).

5) Sensing. Biomimetic EES requires closed-loop control of EES parameters on the basis of real-time monitoring of the ongoing movements, device operations, or motor intentions. The features of each robotic device determine the optimal sensing technologies to synchronize EES with the robot. To meet these device-specific requirements, we selected motion sensors, manual triggers, and force sensors.

5.1) Motion sensors. We integrated inertial measurement units (IMUs) to monitor accelerations and angular velocities across the three spatial directions. These units embed sensor fusion algorithms that integrate inertial and magnetic signals to estimate drift-free measurements of the device orientation with respect to the direction of gravity. These IMUs allowed the detection of robot-assisted movements to synchronize biomimetic EES (Fig. 1B).

5.2) Manual trigger. We designed handheld, appendable ergonomic clickers that captured motor intentions, such as the intention to perform a swing phase of the gait (Fig. 1C).

5.3) Force sensors. We equipped the cranks of a trike with sensors that integrate a dynamometer, gyroscopes, and accelerometers to measure the radial and tangential forces, crank angle, and radial velocity during cycling. These sensors mounted on the cranks captured not only the ongoing phase of the stroke but also the ongoing effort (Fig. 1D). The signals were streamed to the tablet over a low-latency Wi-Fi link (7 ± 4 ms).

This integrated chain of hardware and software components established a wireless neurostimulation platform operating with a latency of 134 ± 26 ms that links the detection of robot-assisted body movements, robotic device operations, and/or motor intentions to the modulation of biomimetic EES programs to activate the neuromuscular system across the various types of existing robotic devices for people with SCI (Fig. 2). In the next section, we demonstrate that this technological framework addressed the challenges involved in the rigorous synchronization of biomimetic EES with the actuation of rehabilitation robotic devices.

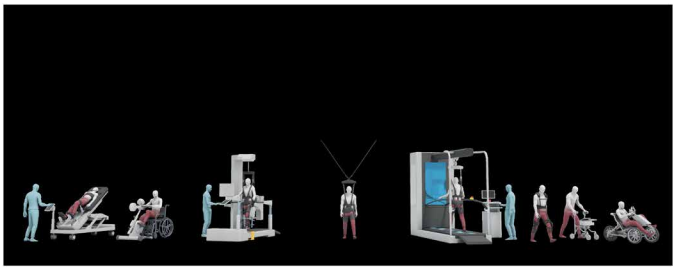

Movie 1. Augmenting rehabilitation robotics with spinal cord neuromodulation.

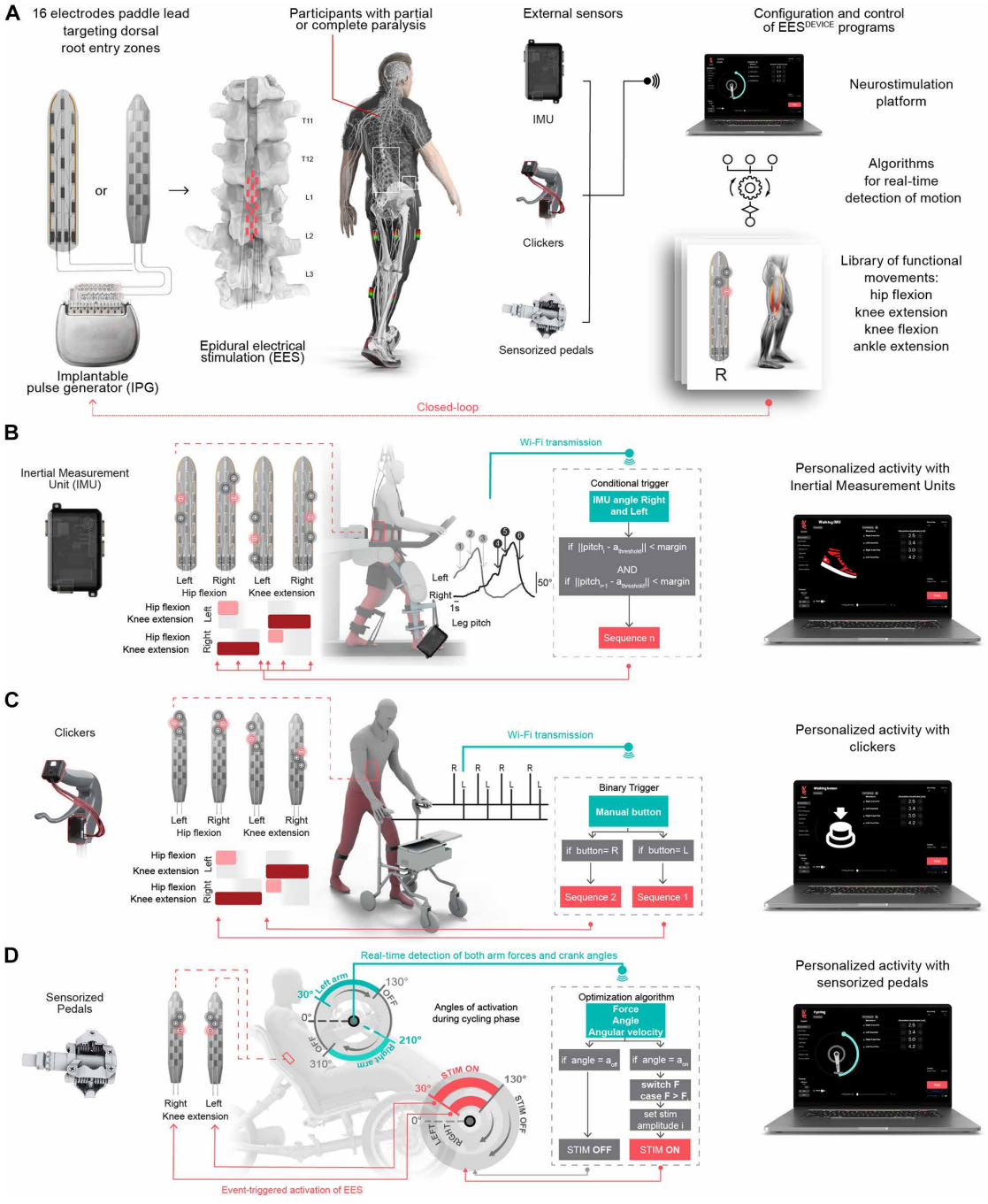

Fig. 1. Closed-loop control of the spinal cord neuroprosthesis. (**A**) Implanted neurostimulation platform that delivers EES through the 16 electrodes incorporated onto two types of paddle leads inserted over the lumbosacral spinal cords of participants with partial or complete paralysis due to SCI. External sensors are used to trigger EES, including IMUs to monitor accelerations and angular velocities across the three dimensions; handheld and appendable ergonomic clickers that capture binary responses linked to a specific motor intent; and crank-mounted sensors that integrate a dynamometer, gyroscopes, and accelerometers to measure radial and tangential forces. The signals from these sensors are streamed to an external processing unit, which consists of a handheld tablet with user-friendly interfaces enabling the configuration and control of EES^{DEVICE} programs. Programs are spatiotemporal sequences of electrode configuration (waveforms), corresponding to functional movements, from a predefined library. Last, the external processing unit sends commands to the implanted neurostimulation platform that delivers EES to close the loop. (**B**) IMUs—Representation of key events detected on the leg IMU signal (1 and 4 start of swing, 2 and 5 midswing, and 3 and 6 end of swing) in an exoskeleton. A threshold-crossing algorithm with adjustable margin for each event that, on the basis of leg angles, triggers the corresponding spatiotemporal stimulation sequence of EES waveforms. (**C**) Handheld and appendable ergonomic clickers. Representation of volitional button clicks triggering independent sequences of EES waveforms that are turned on and off over the course of a duty cycle to support walking. (**D**) Sensorized pedals. Representation of an algorithm detecting the timing of the stroke phase on the basis of the signals from the sensorized pedals. This detection triggers EES waveforms to activate extensor muscles. The amplitude of stimulation is tuned proportionally to the tangential force developed by the participant with both arms.

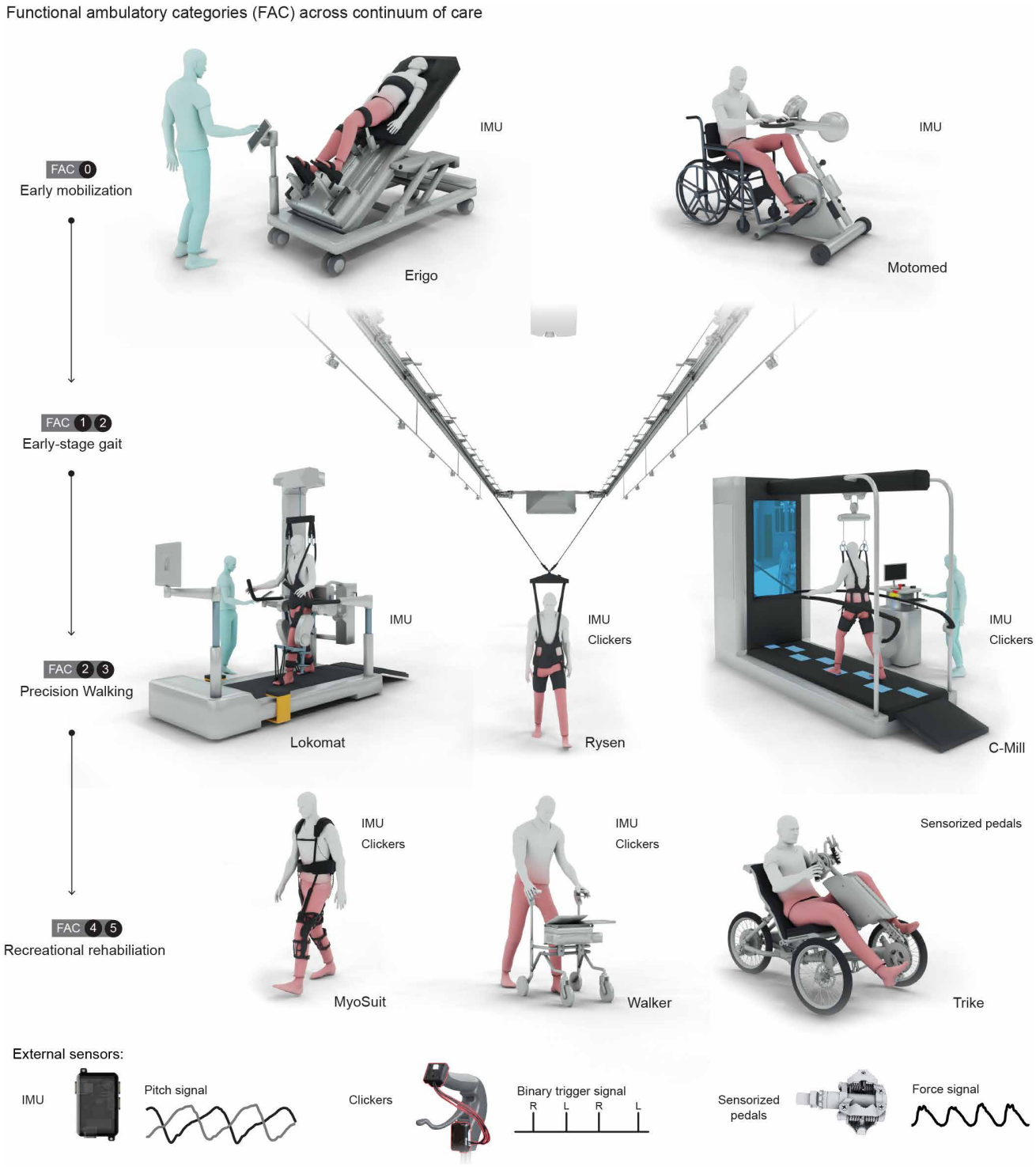

Fig. 2. Rehabilitation robotic devices across the continuum of care. 3D rendering of various robotic devices that are commonly used for lower limb rehabilitation across the continuum of care and that were interfaced with EES in the present study. The devices are ordered from left to right and top to bottom in ascending order on the basis of the categories of FACs that can be addressed with each device. Robotic devices are interfaced with external sensors to synchronize the location and timing of EES with the robotic actuation.

Biomimetic EES augments robot-driven walking

We first asked whether EES could be interfaced with a complex robotic device that provides complete assistance of the lower limbs during body weight–supported stepping on a treadmill (FACs 1 to 3). We selected Lokomat (Fig. 3A) because this device is routinely used for ambulators who are dependent on continuous physical assistance (*32*).

During stepping on a treadmill, healthy individuals display cyclic recruitments of lower limb muscles that are time locked to key gait events. To capture this timing, we developed an orientation estimation algorithm based on the IMUs. We first verified the robustness of the algorithm. For this, we mounted an IMU onto a circular disc with a position-controlled motor encoder that provided ground truth orientation. After 15 min of continuous data streaming, the mean error amounted to 2.21°, whereas the drift between IMUs and the encoder was limited to 0.19°, showing that the algorithms exhibited negligible drifts across time and movement speeds. Quaternions yielded by the algorithm were converted to user-interpretable Euler angles (roll, pitch, and yaw) using a convention that avoided singularities in the primary axis of rotation. We detected gait events on the basis of a threshold-crossing algorithm with adjustable margins that maintained stability of detected events despite potential delayed or dropped data packets.

We then programmed $EES^{LOKOMAT}$. To reproduce the muscular activity associated with walking, it is imperative to detect swing, midswing, and stance events, because the onset and/or end of muscle activity coincides with these events (Fig. 1B). We found that IMUs placed on the left and right shanks led to the most accurate detections (Fig. 3B). $EES^{LOKOMAT}$ remained synchronized to the gait cycle over the tested range of treadmill speeds, from 1.2 to 2.6 km/hour (Fig. 3C).

We tested $EES^{LOKOMAT}$ in two individuals with partial (P1) and complete (P5) SCI. Passive movements of the lower limbs driven by the gait orthosis led to weak levels of muscle activity (Fig. 3, D and E). $EES^{LOKOMAT}$ augmented the recruitment of lower limb muscles and improved the timing of muscle activity (Fig. 3E). This robust activation led to improved gait performance, which was reflected in the reduction in interaction forces with Lokomat (Fig. 3F). This reduction revealed that the participants contributed actively to the motion, requiring less assistance from the gait orthosis.

Physiotherapists were asked to determine the optimal level of body weight support (BWS) for stepping, as judged by the maximum weight bearing that still allows fluid lower limb movements. Compared with the condition without $EES^{LOKOMAT}$, they selected a substantial decrease in the level of BWS during $EES^{LOKOMAT}$ (P1, 42 to 20% BWS; P5, 78 to 51% BWS) (Fig. 3G).

We also asked whether biomimetic EES could engage the neuromuscular system with Erigo (*33*), which also moves the lower limbs along predefined paths on a motorized tilt table (FACs 0 to 2). To ensure the stability of detection algorithms despite changes in body orientation and speed, we merged signals from IMUs attached to the tilting structure and lower limb actuators (fig. S1, A and B). Participants with partial or complete paralysis who exhibited no or negligible activity in lower limb muscles during passive lower limb movements showed substantial and well-timed muscular activity when EES^{ERIGO} was turned on (fig. S1, D and E). These results demonstrate the possibility to leverage biomimetic EES to augment the activation of the neuromuscular system during walking with robotic devices that provide complete assistance of lower limb movements.

Biomimetic EES enables unrestricted walking with robot-assisted balance

Multidirectional robotic BWS systems enable natural overground walking in people with gait impairments, but these systems cannot be used by people with paralysis. We thus aimed to illustrate that biomimetic EES can be interfaced with these systems to enable natural overground walking (FACs 1 to 3).

We selected Rysen (Fig. 3H) because this system provides adjustable assistance along the three Cartesian directions during walking in a large workspace (*34*). We configured a gravity assist (*13*, *35*), which consisted of selecting the optimal forward and upward forces constantly applied to the trunk by Rysen to walk over ground.

Volitional walking requires initiating the swing phase of the gait with a precise timing. To empower our participants with this precision, we detected motor intentions using the ergonomic clickers held in their hands. Two clickers enabled the participants to trigger a sequence of EES waveforms that engaged the contralateral flexor muscles to facilitate the left or right swing phases (Fig. 3I). Evaluations of this strategy in two participants with paralysis showed that the safe environment enabled them to walk over ground hands free.

Given that the objective of rehabilitation with systems such as Rysen is to promote coordinated movements between the upper and lower limbs, we also sought to synchronize EES^{RYSEN} on the basis of IMUs attached to each arm (fig. S2A). This strategy enabled walking with a tight coupling between the upper and lower limb movements.

We reasoned that these strategies may also enable participants to accommodate step placements to environmental constraints. These visually guided walking movements can be trained using robotic systems equipped with augmented reality, such as C-Mill, which provides BWS while targets are projected onto the treadmill belt to inform the patient of the expected foot placements (fig. S2B). $EES^{C\text{-}MILL}$ allowed participants with partial or complete paralysis to place their feet with high accuracy on the virtual targets projected on the treadmill belt, reaching a performance accuracy as high as 92% for a succession of 70 steps (fig. S2C).

Biomimetic EES augments robot-assisted cycling

We then asked whether EES could be configured to activate the neuromuscular system during rehabilitation on a physical therapy exercise bike, such as MOTOmed (fig. S3A). Because the attachment of the feet onto the cranks imposes a perfect coupling between the oscillations of the right and left lower limbs, we used a single sensor to synchronize EES to the duty cycle (fig. S3A). $EES^{MOTOMED}$ operated with an acceptable angle detection error (<15°) across cycling speeds ranging from 15 to 60 rpm (fig. S3B). In the absence of EES, MOTOmed failed to elicit muscle activity during passive movements of the lower limbs. Instead, $EES^{MOTOMED}$ promoted the rhythmic recruitment of left and right knee extensor muscles with a timing that matched the natural activity of these muscles recorded in able-bodied people (fig. S3C). This activity produced a peak acceleration at the feet that generated a force against the pedal (fig. S3D). Contrary to the muscle exhaustion observed during FES of muscles (*36*–*38*), $EES^{MOTOMED}$ promoted sustained muscle activity over the entire duration of a 1-hour cycling session at 20 to 30 rpm (fig. S3E). Moreover, $EES^{MOTOMED}$ does not require cumbersome preparations to position electrodes and wires on patients before each rehabilitation session.

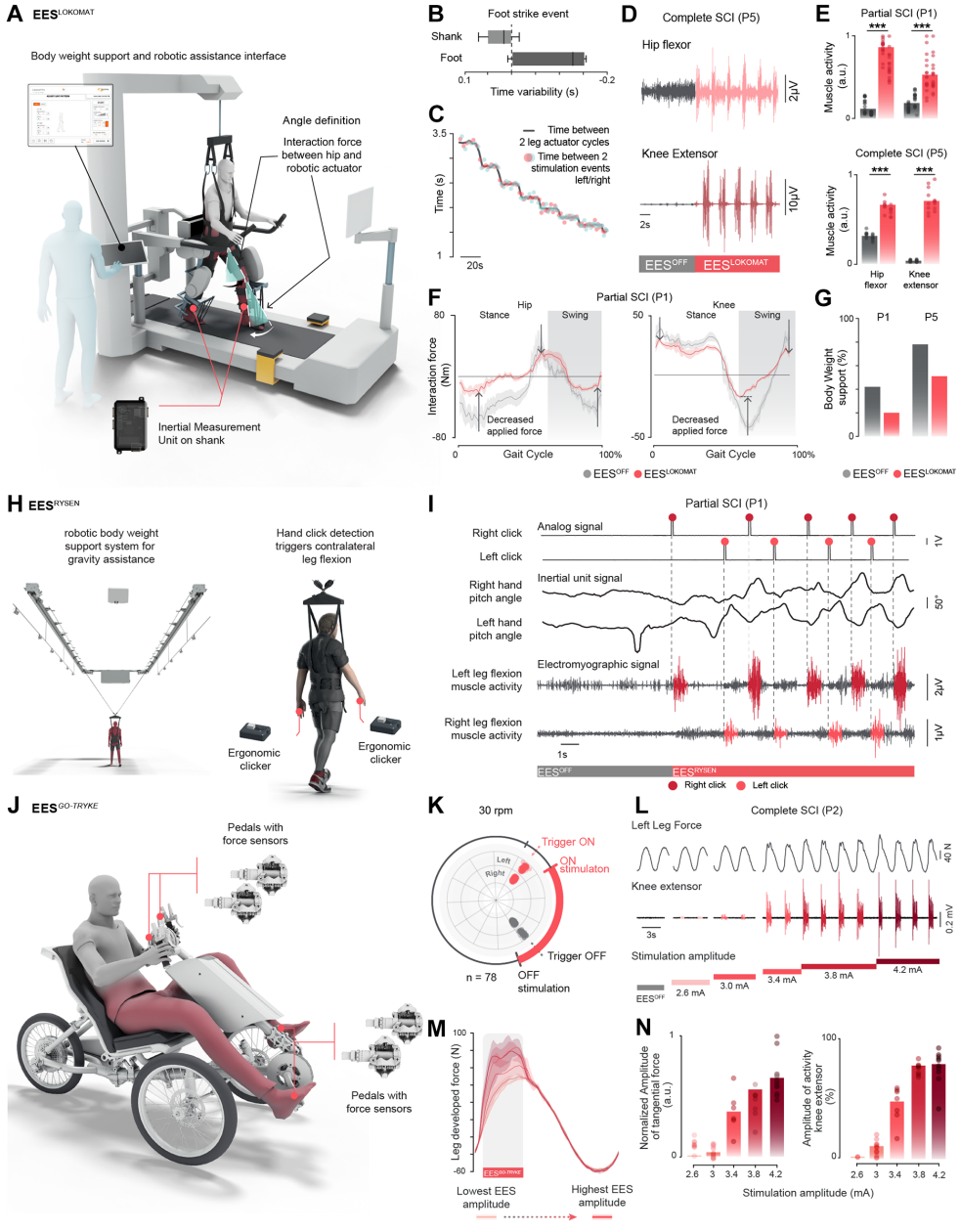

Fig. 3. Synchronization and augmentation of rehabilitation robotic devices with biomimetic EES. (**A**) Integration of IMU sensors to the leg actuators of Lokomat. (**B**) Time difference in the foot strike event detection when placing the IMU on the shank (light gray) or on the foot (dark gray), with regard to ground truth defined by insole force sensors. (**C**) Plot representing the synchronicity of the time between two consecutive cycles of the leg actuators and two consecutive swing-related triggering events for the left and right body sides across increasing stepping speeds. (**D**) Activity of the left hip flexor and knee extensor muscles over 10 consecutive steps for P5. (**E**) Bar plot reporting muscle activity for the hip flexor and knee extensor muscles from both body sides in P1 and P5. For P1, $P = 1.06 \times 10^{-6}$ (left/right flexors, left extensor), $P = 4.37 \times 10^{-6}$ (right extensor), $N = 16$; for P5, $P = 5.83 \times 10^{-4}$ (all flexors and extensors), $N = 7$ (Mann-Whitney U test); $^{***}P < 0.001$. (**F**) Average interaction forces between participant P1 and the robotic leg actuators over a gait cycle with 60% robotic assistance. The locations of the interaction forces are schematized in (A). Interaction forces closer to 0 represent a decrease in the force applied by the robotic actuators to the lower limbs. (**G**) Bar plot reporting BWS for optimal gait rehabilitation training conditions that were determined by the physiotherapist. (**H**) Robotic BWS system that provides multidirectional assistance during walking in a large workspace. EES waveforms are triggered on the basis of ergonomic clickers that are handheld by the participants for hands-free walking. (**I**) Examples of events detected by a click on ergonomic clickers to trigger contralateral swing-related EES waveforms are shown together with the concomitant recordings of EMG activity from leg flexor muscles and left/right hand pitch angle traces. (**J**) Schematic representation of the recumbent trike onto which we mounted four sensors to measure forces generated by both arms and legs and the oscillations of the shank. (**K**) Diagram showing onset (red) and offset (gray) events for both legs, with stimulation periods highlighted in red. It indicates the angles for receiving stimulation and sending commands, accounting for a 134-ms delay at 30 rpm ($N = 78$). (**L**) Tangential forces produced by the leg concomitantly with the muscle activity recorded from knee extensor muscle for the five levels of stimulation amplitudes of P2. (**M**) Tangential forces produced by the leg during the stroke phases at five different levels of stimulation amplitudes. (**N**) Bar plots reporting tangential forces produced by the leg and the amplitude of activity from knee extensor muscles for the five different levels of stimulation amplitudes ($N = 49$). a.u., arbitrary units.

We lastly aimed to provide participants with adaptive control over the relative activation of muscles during cycling. We selected Go-Tryke, which is an electrically assisted, recumbent trike that leverages upper and lower limb cycling movements to enable people with reduced ambulatory capabilities to enjoy bike rides outdoors (Fig. 3J). We equipped Go-Tryke with pedals that allow for embedded accelerometers, gyroscopes, and force sensors (Fig. 3J). These signals allowed us not only to detect the onset of stroke movements but also to monitor the contribution of upper and lower limbs to force production. We designed an algorithm that integrated these signals to anticipate stroke onsets with phase delays that scaled with the speed of cycling movements (Fig. 3K). These detections triggered EES waveforms that engaged knee extensor muscles ($EES^{GO\text{-}TRYKE}$). In addition, we injected a proportional controller into the detection algorithm, which scaled the amplitude of $EES^{GO\text{-}TRYKE}$ with the degree of effort detected from the combined forces of both upper limbs (Fig. 3L).

$EES^{GO\text{-}TRYKE}$ enabled graded control over the amplitude of knee extensor muscles (Fig. 3, M and N). Enhanced muscle activity translated into a proportional increase in the force produced by the lower limbs. These results demonstrate the possibility of leveraging biomimetic EES to augment the activation of the neuromuscular system during robot-assisted cycling.

Device-agnostic implementation by nonexpert users

Given that the seamless implementation of the system across devices was a desired feature of the system, we developed a guideline and interface for nonexpert users and then sought to perform a formal evaluation of this feature. We asked three physiotherapists with no engineering background to configure EES^{DEVICE} for diverse rehabilitation exercises. The flexibility and ergonomics of this technological platform combined with the robustness of the algorithmic framework enabled the three physiotherapists to configure EES^{DEVICE} within 2 to 10 min, depending on the device. We also provided the simplified version of the interface to configure and control the system to study participants. These technologies have now been operated by these participants for more than 2 years with positive feedback and without a report of serious adverse events.

Robot-assisted rehabilitation augmented by EES promotes neurological recovery

We next aimed to evaluate the effects of rehabilitation enabled by the augmentation of robotic assistance with biomimetic EES in people with chronic SCI (FACs 0 to 3). We enrolled four participants with partial (P1) and motor complete (P2, P4, and P5) SCI (table S1) who had previously undergone robot-assisted rehabilitation using Lokomat and/or MOTOmed because their neurological status did not permit lower limb rehabilitation in other conditions. Despite these extensive rehabilitation programs (Fig. 4, A to C), participants did not show improvement in their neurological conditions, as quantified by the absence of changes in lower limb motor scores. Most of them had remained completely paralyzed, as quantified by the null motor scores.

These participants engaged in a rehabilitation program (*4*) during which they underwent daily sessions of walking and cycling enabled by biomimetic EES and various robotic devices (Fig. 4, A and B). Although biomimetic EES restored coordinated patterns of muscle activity in all four participants with partial or complete paralysis, the stimulation alone was insufficient to support walking without additional robot-assisted balance. The need for this additional robotic assistance declined over time (Fig. 4E). Eventually, the four participants regained the ability to walk over ground with EES alone, only requiring a rollator for balance maintenance. Assessment of neurological status without EES after this rehabilitation program revealed that all four participants with chronic SCI exhibited an increase in lower limb motor scores (Fig. 3, C and D).

These results showed that a period of rehabilitation assisted with robotic devices alone was not sufficient to promote improvement in the neurological status of patients with chronic SCI. In the early stage of rehabilitation, EES alone was also insufficient to enable walking and cycling. Instead, the combination of robotic assistance and biomimetic EES enabled intensive and safe rehabilitation of the participants, which restored volitional control over previously paralyzed muscles even when EES was turned off.

Recreational rehabilitation and activities

Last, we aimed to document the possibility of augmenting robot-assisted recreational activities at home and outdoors with biomimetic EES (FACs 4 and 5). Lower limb exoskeletons can compensate for weak knee extensions during standing and walking. For example, Myosuit (*39*) is a lightweight, soft exoskeleton that actively supports weight bearing via a tendon cable assisting knee and hip extension. EES enables walking in people with complete paralysis, but these individuals can show difficulties in achieving full weight-bearing standing and walking. We reasoned that Myosuit could provide the necessary additional support to improve walking in these individuals.

To synchronize EES with Myosuit, we triggered EES waveforms based on IMUs attached to each shank (Fig. 5A). As expected, $EES^{MYOSUIT}$ increased the degree of knee and hip extensions in the two tested participants with partial or complete paralysis. Improved knee and hip extension translated into a more upright posture (Fig. 5B). These improvements led to enhanced balance and standing capacities and enabled an increase in walking speed (Fig. 5C).

We also asked whether EES could be interfaced with assistive devices to enable nonambulatory patients with partial or complete SCI to ambulate outdoors on natural terrains, including stairs (FAC 5). For this purpose, we interfaced the clickers with two types of assistive devices. First, we mounted two custom-made clickers onto an all-terrain rollator designed to support ambulation over the broad range of surfaces encountered in ecological settings. Each clicker was linked to the onset of EES waveforms promoting the swing phase of contralateral lower limbs ($EES^{ROLLATOR}$) (Fig. 5D). Second, we integrated both clickers onto the same hand grip of a crutch to enable the participants to trigger the swing phase of the left and right lower limbs from the same hand (EES^{STAIR}). This configuration released the other hand, which was free to hold a handrail to walk along stairs (Fig. 5F).

Using these devices, participants with partial and complete paralysis could walk outdoors on terrains covered with gravel, grass, or snow. They were also able to climb up and down stairs (Fig. 5G). Two participants were able to enroll in running competitions that aimed to collect funds for not-for-profit foundations. One of the participants with partial paralysis raced for a total of 4 hours, completing a total of 4069 steps during this period (Fig. 5E).

We lastly asked whether $EES^{GO\text{-}TRYKE}$ could augment recreational rides with the Go-Tryke in ecological settings (Fig. 5H). Given

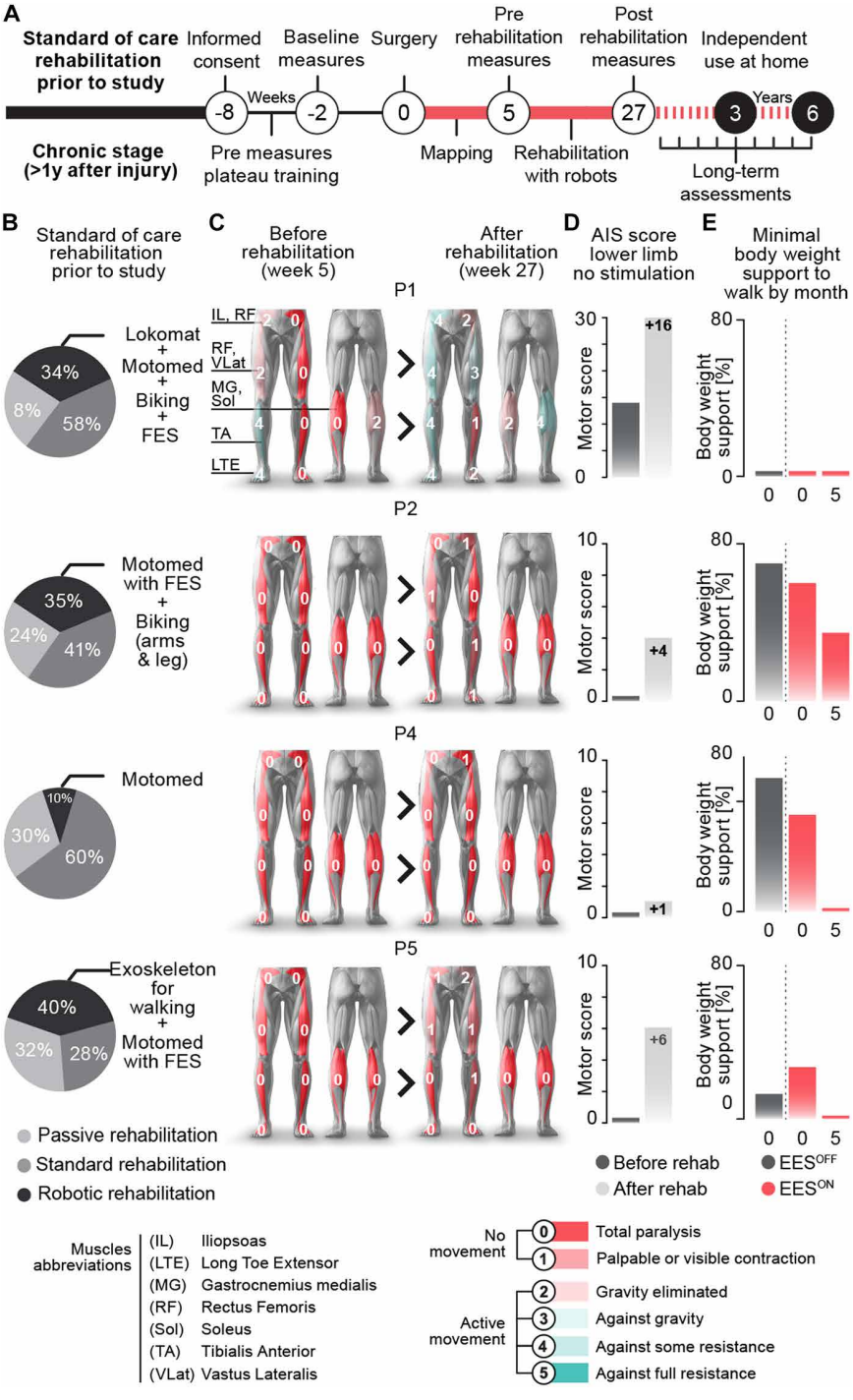

Fig. 4. Robot-assisted rehabilitation augmented by EES promotes neurological recovery. (**A**) Timeline of STIMO during the first months (white) of the trial and subsequent years (black) (NCT02936453). (**B**) Pie charts representing the percentage of hours performing passive (stretching and massage), standard (classical physiotherapy, ergotherapy, and sports), and robot-assisted rehabilitation (walking exoskeleton and BWS, MOTOmed with optional FES, and biking on Giger MD or Trike with mechanical coupling) before enrollment in the STIMO clinical trial for each participant. (**C**) Body schemes report the lower extremity motor score (LEMS) measured before and after rehabilitation with ESS in combination with robotic devices. The AIS score is performed in the absence of stimulation. (**D**) Relative changes in the LEMS of the AIS score measured before and after rehabilitation with ESS in combination with robotic devices. (**E**) Bar plots report the evolution of the required amount of BWS (percentage of body weight) necessary to enable each participant to walk independently over the period of rehabilitation with EES.

that EES$^{GO\text{-}TRYKE}$ includes a proportional controller that scales the amplitude of stimulation with the degree of effort detected from the combined forces of both upper limbs, we anticipated that EES$^{GO\text{-}TRYKE}$ could adjust the contribution of lower limb extensor muscles to the ongoing requirements of the terrain and intentions of the user. Concretely, the algorithm interpreted the augmentation of tangential forces generated by the upper limbs as an increase in effort and, therefore, as the need for additional propulsive forces. This scenario typically occurred when cycling uphill or when the user desired to increase the speed (Fig. 5I).

EES$^{GO\text{-}TRYKE}$ enabled real-time control over the amplitude of knee extensor muscles, which translated into a proportional increase in the force produced by the lower limbs. These adaptations allowed long-lasting rides with Go-Tryke over varied and challenging outdoor terrains (Fig. 5J). The participant reported a natural and pleasant coupling between their effort and the engagement of the lower limb neuromuscular system. These results demonstrate the neuroprosthetic integration of biomimetic EES with robotic devices to support recreational walking and cycling outdoors in people with SCI.

DISCUSSION

EES has demonstrated potential to augment neurological recovery in people with paralysis (*5*, *21*–*23*), but EES alone can be insufficient to support independent ambulatory activities in the early stage of the therapy or in people with severe paralysis. We thus reasoned that rehabilitation robotics may complement EES. Consequently, we developed a flexible technological framework to address the challenges involved in the integration of activity-dependent biomimetic EES with robotic devices that are now used in rehabilitation centers to promote exercise in people with motor impairments or to support activities of daily living in people with paralysis. We provide the first preliminary evidence that this framework may be sufficient to ensure the safe and rigorous synchronization of biomimetic EES with the actuation of robotic devices. This integration did not require modifying the controllers of the robotic devices or accessing the features of robotic actuation. Therefore, our strategy was agnostic to the specific features of the robotic device. Nonexpert physical therapists and study participants were able to configure and use EES with any tested robotic device. Here, we discuss how these preliminary results suggest that augmenting rehabilitation robotics with EES may enhance the functional recovery of people with SCI. However, we also point out the need for additional developments to

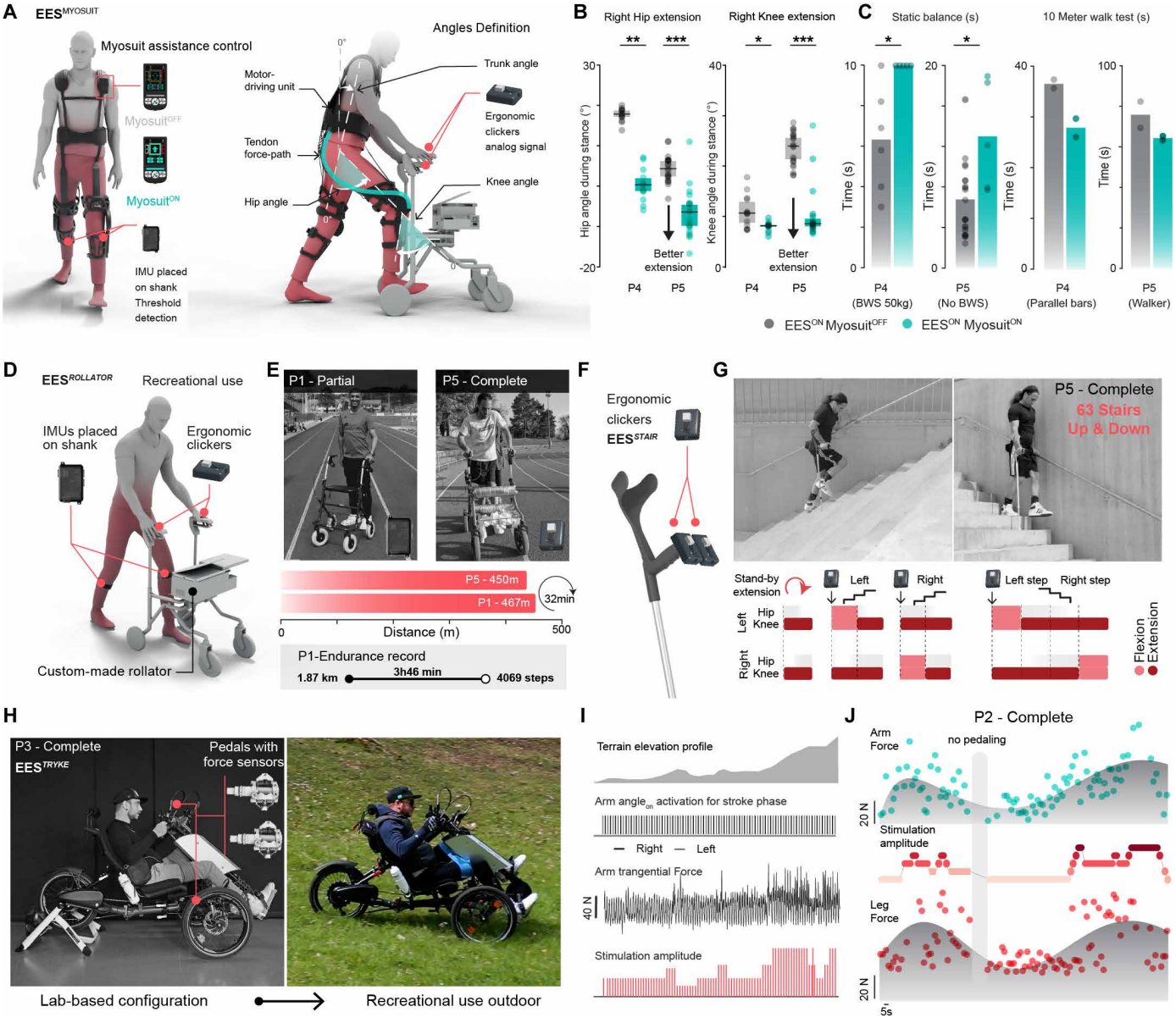

Fig. 5. Recreational rehabilitation and activities with biomimetic EES. (**A**) Lightweight, textile-based gait orthosis actuated through tendon force, termed Myosuit. Ergonomic clickers or IMUs attached to the shank are used to synchronize $EES^{MYOSUIT}$ with the movement of the lower limbs. The assistance of the orthosis can be enabled or disabled directly on the device through a remote control located by the shoulder. (**B**) Boxplots reporting quantifications of maximal hip and knee extensions on the basis of conventions depicted in (A) during walking with $EES^{MYOSUIT}$ without and with exoskeleton assistance for P4 and P5. For P4, $P = 6.66 \times 10^{-9}$ (hip extension), $P = 2.439 \times 10^{-3}$ (knee extension), $N = 13$; for P5, $P = 5.60 \times 10^{-6}$ (hip extension), $P = 1.37 \times 10^{-6}$ (knee extension), $N = 21/34$ (off/on) (Mann-Whitney U test); $^{*}P < 0.05$, $^{**}P < 0.005$, and $^{***}P < 0.001$. (**C**) Bar plots reporting standing capabilities without and with exoskeleton assistance for 10- or 20-s balance tests for P4 with 50-kg BWS and without BWS for P5. For P4, $P = 0.0152$, $N = 6/5$ (off/on); for P5, $P = 0.03572$, $N = 18/5$ (off/on) (Mann-Whitney U test); $^{*}P < 0.05$. (left). Bar plots reporting durations of the 10-m walk tests performed between parallel bars for P4 and with a walker for P5. (**D**) Custom-made rollator, including charging station, control interface, and mounted ergonomic clickers. $EES^{ROLLATOR}$ is synchronized on the basis of clickers or IMUs attached to the shank. (**E**) Photographs showing participants P1 and P5 during world-wide races to fight paralysis, setting personal (P1) and Guiness Book world (P5) records. (**F**) Crutch mounted with two ergonomic clickers that enable the participant to trigger bilateral EES^{STAIR} with one hand while holding the ramp with the other hand. (**G**) Photographs showing P5 climbing up and down a staircase with 63 steps in outdoor settings. The spatiotemporal sequence of stimulation involved in EES^{STAIR} is shown at the bottom, combining the alternation between EES waveforms targeting knee extensor muscles to stand and hip and ankle flexor muscles to raise the foot and generate a swing phase. (**H**) Photographs illustrating the translation from lab-based configurations to ecological use for recreational activities of P3. (**I**) From top to bottom: Elevation profiles of the terrain, detection of the stroke phases, tangential forces produced by both arms, and amplitude of stimulation. The stronger the forces produced by the arms are, the higher the amplitude of the delivered stimulation, thereby proportionally supporting the detected effort. (**J**) Relationships between tangential forces produced by the arms and changes in stimulation amplitude and associated tangential forces produced by the legs during cycling over an outdoor terrain with hills, the profile of which is depicted approximately by the gray envelope ($N = 220$).

fulfill this therapeutic potential that must be demonstrated in sufficiently powered clinical trials.

Gait rehabilitation aims to promote activity-dependent reorganization of the nervous system to enhance neurological recovery (*4*, *6*, *7*). A large number of robotic devices have been developed and commercialized to facilitate gait rehabilitation, each providing an environment that is optimized for the current neurological status of the patients (*8*–*14*). Although these devices are useful for promoting activity-dependent modulation of proprioceptive pathways, they showed limited efficacy to engage the dormant neuromuscular system of patients with neurological disorders (*20*). Consequently, they do not take full advantage of activity-dependent mechanisms to augment recovery (*8*). Complementary neuroprosthetic strategies have been considered to augment rehabilitation robotics. For example, FES of muscles has become a common solution to engage specific groups of muscles during rehabilitation, but this methodology presents several inherent limitations that restrict its efficacy and appeal (*19*, *20*, *37*). More recently, a spinal cord stimulation was applied externally to facilitate muscle activity during exoskeleton-assisted walking (*40*). However, the location and timing of the stimulation were not synchronized with the ongoing movements, and consequently, the overall activation of the neuromuscular system remained limited. Here, we show that activity-dependent biomimetic EES triggered the immediate, robust, and sustained activation of the neuromuscular system in people with partial or complete paralysis due to SCI who exhibited quiescent muscle activity without EES. Moreover, biomimetic EES was effective to engage the neuromuscular system across multiple types of robotic devices that each required specific strategies to synchronize EES with robotic actuations or motor intentions.

We also provide preliminary results on the complementarity between robotic devices and biomimetic EES to support rehabilitation. Rehabilitation robotics alone showed no or limited efficacy to improve recovery in our participants with chronic SCI. These negative outcomes are consistent with the overall conclusion from meta-analyses that highlighted no additional benefits of robot-assisted rehabilitation compared to conventional rehabilitation for neurological recovery (*41*–*43*). Similarly, EES alone could restore standing and basic walking movements, but the participants with SCI were not able to perform these activities without robotic assistance in the early phases of rehabilitation. Therefore, the complementarity between EES and robotics was essential to support early-stage rehabilitation in people with SCI. The essential contribution of robotic devices declined over time, and eventually, participants could stand and walk independently with biomimetic EES alone or with more transparent robotic assistance. This recovery coincided with improvements in the neurological status of the participants. These results suggested that augmenting rehabilitation robotics with biomimetic EES steered activity-dependent reorganization of the nervous system (*4*, *6*, *7*), although the specific contribution of robotic devices in this reorganization remains unclear and will require further studies. We anticipate that commonly used rehabilitation robotic systems may facilitate the implementation of EES in the early stage of the intervention, when EES alone is not sufficient to enable robust standing and walking. The combination of robotic devices and EES could therefore play an important role in augmenting the neurological recovery of patients with subacute and chronic SCI (*29*, *31*, *44*, *45*). In the present study, we introduced a framework that illustrates how to simplify the combination of these two therapeutic modalities, given that our framework can be easily deployed across rehabilitation centers and only requires the supervision of physical therapists. Although rehabilitation robotics may not augment neurological recovery per se, these systems have become the standard of care, because they enable the practical and consistent delivery of rehabilitation for individuals with various ranges of paralysis. This combination is therefore appealing, because the various robotic systems used in our study have become common assistive devices to support rehabilitation across the continuum of care in treatment centers worldwide. Although these results are encouraging, future studies will have to demonstrate the synergy between robotic devices and EES in a sufficiently powered clinical trial, as well as the biological mechanisms supporting this synergy.

We delivered device-specific EES programs using a repurposed neurostimulation platform that was originally developed to deliver continuous deep brain stimulation. To enable real-time control of EES, we conceived a wireless bridge between the control computer and the neurostimulation platform. Although this bridge allowed us to demonstrate the possibility to interface EES with rehabilitation robots, the necessity of multiple communication methodologies precludes the large-scale deployment of comparable strategies. It is therefore essential to design purpose-built technologies that allow patients and physical therapists to configure and use rigorously synchronized biomimetic EES safely through practical interfaces, smart phones, and voice-controlled watches. Moreover, this purpose-built neurostimulation platform must resolve the limitations of current technologies, providing the possibility to configure stimulation ramps, independent stimulation frequencies, and high-frequency stimulation bursts that will greatly augment the influence of EES on the facilitation of movement.

The putative complementarity between robotics and EES provides preliminary results that should encourage innovations in the field of rehabilitation robotics and neuroprosthetics to augment the recovery of mobility and upper limb functions in people with SCI (*46*, *47*). Moreover, the same complementarity may contribute to the recovery of people with other neurological conditions, such as Parkinson's disease (*48*) and stroke (*49*).

MATERIALS AND METHODS

Clinical study

Study design and participants

All experiments were carried out as part of the ongoing clinical feasibility study STIMO (Stimulation Movement Overground), which investigates the effects of EES with robot-assisted rehabilitation in patients with SCI (https://clinicaltrials.gov/ct2/show/NCT02936453). This study was approved by the Swiss ethical authorities (CER-VD no. 04/2014 PB_2016-00886, Swissmedic ProjectID 10000234, previous SMC-Nr. 2016-MD-0002) and was conducted in accordance with the Declaration of Helsinki. Nine individuals were implanted and finished the main part of the study. We report here the results of EES combined with robotics in five of the nine individuals. Intensity and diversity of rehabilitation programs before the STIMO study were collected as part of their medical history. Their neurological status was evaluated according to the International Standards for Neurological Classification of Spinal Cord Injury (*50*), is reported in table S1, and was previously described (*4*, *29*, *31*). All participants signed a written informed consent before their participation and at each approved amendment throughout the study. Patients followed a

5-month rehabilitation program personalized on the basis of the participants' improvements. After the main phase of the study, participants were suggested the possibility to join a follow-up study for a maximum of 6 years during which they could continue using the stimulation. Data collection was performed during sessions dedicated to stimulation optimization either at Lausanne University Hospital (CHUV, Lausanne, Switzerland), at Revigo Rehabilitation Center (Volketswil, Switzerland, part of Rehaklinik Zihlschlacht AG), or outdoors.

Inclusion criteria

The following inclusion criteria were applied for study enrollment: age 18 to 65 (women and men); sensorimotor or motor complete and incomplete SCI graded as American Spinal Injury Association (ASIA) Impairment Scale (AIS) A, B, C, or D; level of lesion of T10 and above based on the AIS level determination by the PI; preservation of conus function; intact distance between the cone and the lesion of at least 60 mm; focal spinal cord disorder caused by either trauma or epidural, subdural, or intramedullary bleeding; minimum of 12 months postinjury; completed in-patient rehabilitation program; for AIS C and D, ability to stand with walker or two crutches; stable medical, physical, and psychological condition as considered by the investigators; ability to understand and interact with the study team in French or English; adequate caregiver support and access to appropriate medical care in patient's home community; agreement to comply in good faith with all conditions of the study and to attend all required study trainings and visits; and agreement to participate in two training sessions before eligibility was confirmed and to provide and sign an informed consent form before any study-related procedures.

Exclusion criteria

Individuals were excluded on the basis of any one of the following criteria: limitation of walking function based on accompanying (CNS) disorders (systemic malignant disorders, cardiovascular disorders restricting physical training, and peripheral nerve disorders); history of significant autonomic dysreflexia, cognitive/brain damage, epilepsy, spinal canal stenosis, and the use of an intrathecal baclofen pump; any active implanted cardiac device, such as a pacemaker or defibrillator; any indication that would require diathermy; any indication that would require magnetic resonance imaging; an increased risk of defibrillation; severe joint contractures disabling or restricting lower limb movements; hematological disorders with increased risk for surgical interventions (increased risk of hemorrhagic events); participation in another locomotor training study; congenital or acquired lower limb abnormalities (affection of joints and bone); women who were pregnant (pregnancy test obligatory for a woman of childbearing potential), breast feeding, or not willing to take contraception; known or suspected noncompliance; drug or alcohol abuse; spinal cord lesion due to either a neurodegenerative disease or a tumor; other anatomic or comorbid conditions that, in the investigator's opinion, could limit the patient's ability to participate in the study or to comply with follow-up requirements or affect the scientific soundness of the study results; or a patient who was unlikely to survive the protocol follow-up period of 12 months.

Electrical epidural stimulation delivery

Neurostimulation system

The neurostimulation system has been previously described (*29*). EES was delivered with an IPG (Medtronic Activa RC) connected through lead cables to a paddle lead (either Specify 5-6-5 from Medtronic used for treatment of chronic pain or a new paddle lead developed by ONWARD Medical). This system enables monopolar and multipolar stimulation at a constant current through one or a subset of the 16 electrodes of the paddle lead or the case of the IPG (anode). The IPG was modified from its clinical version with investigational firmware that enabled real-time communication with software running on an external tablet computer (NEUWalk Research Programmer Application—NRPA, model 09103, Medtronic). EES commands were sent by the control software (described below) through the NRPA to the IPG. The NRPA then communicated wirelessly with the IPG.

Interactive software application for stimulation control

Custom software was developed (Windows Presentation Foundation App, C#, .NET Framework 4.5.2) to provide an intuitive way for patients, caretakers, physiotherapists, or rehabilitation doctors to select a predetermined stimulation program associated with a rehabilitation exercise and modify the stimulation amplitudes within clinician-determined limits. The software interfaced with the neurostimulation system over Bluetooth using the NRPA and implemented a wireless sensor module over Wi-Fi that enabled stimulation delivery in a closed loop.

The stimulation programs were composed of a precise temporal sequence of multiple stimulation blocks, with a maximum of four blocks in parallel. Each stimulation block was defined by a specific selection of cathodes and anodes on the lead and IPG and aimed to produce a targeted function by stimulating a dedicated dorsal root. At any given moment, stimulation was delivered at a single frequency; however, a high-frequency recruitment could be mimicked by a stimulation block that delivered doublets or triplets, i.e., two or three pulses spaced by 2 ms. A graphical user interface was developed to facilitate the creation, modification, and fine-tuning of the stimulation programs by a trained expert. The software was part of the investigational system of the clinical study and was developed in accordance with the IEC-62304 standard for class A medical device software and with the use of versioning and an automated unit test framework. A risk management file was developed for the full investigational system from which other risk mitigations were defined. Any changes to the software or other components led to a verification and validation (V&V) cycle of the system and a resubmission of the amended study protocol to the competent authority and ethics committee. To maximize the number of bug fixes and features in each iteration of the software, we modularized its structure and updated our V&V methods. We created a dedicated module in the software responsible for closed-loop stimulation control that read the sensor input, applied motion detection algorithms, and output stimulation events. This module could then be updated while minimizing the impact to the rest of the software. We then implemented a surrogate for EES that could be used to test the system on unimpaired individuals during our V&V cycle.

Multipurpose IMU and ergonomic clickers

The wireless sensor module of our software application was a compact IMU with dimensions of 56 mm by 39 mm by 18 mm and a weight of 46 g (next-generation IMU, x-io Technologies). It combined onboard sensors and data processing algorithms that stream a selection of acceleration, angular velocity, and quaternions over Wi-Fi at a maximum of 100 Hz. In addition, analog inputs could be combined to the data stream via a dedicated Molex PicoBlade header. The sensor platform implemented configuration and streaming using the Open Sound Control protocol over user datagram protocol.

Acceleration and angular velocity were used to estimate the orientation of the sensor in quaternion representation. The latter was then converted to Euler angles to facilitate interpretation by the users. Twelve unique translations from quaternions to Euler angles existed, and two were selected as relevant for the sensor placement in our applications. These were selected precisely to avoid discontinuities in the calculated pitch. The performance of the AHRS (Attitude and Heading Reference System) data fusion algorithm was evaluated on a custom test bench. Dedicated mechanical clickers were designed and connected to the sensor via the analog inputs to provide a mechanism for detecting a button press. The clickers were fitted with a debounce electronic circuit to limit noise at the source.

Closed-loop stimulation paradigms

Event detection

To deliver the correct stimulation at the correct time during exercise execution, closed-loop stimulation paradigms were developed on the basis of input from the wireless sensor module. The sensor was fixed in a position where relevant motion was captured, for example, on the shanks for gait training. The orientation of the sensor, namely, the pitch, was used to detect key motion events, such as foot-off, using a thresholding algorithm. In addition, the sensor integrated a button sending an analog binary signal. The triggering of each event activated a predetermined stimulation sequence that aimed to support a dedicated movement. A refractory period (50 to 150 ms) was defined after each trigger event to avoid unwanted retriggering of the same event.

Thresholding algorithm

The number of motion events and their threshold values were customizable and could be set to trigger an ascending or descending signal crossing of a dedicated sensor's pitch. The threshold crossing algorithm was implemented to work robustly across a signal from 0° to 360° and included a margin around the threshold within which two subsequent samples must be located. This ensured that an event was triggered only when the limb was in proximity of the expected biomechanical state. For example, no stimulation would occur if the limb was moving too fast or if data packets were dropped.

Control algorithms

Gait training was supported in a closed loop by placing one sensor on each leg, either on the foot or shank—EES^{GAIT}. An initial attempt to perform a swing phase could then trigger a flexion stimulation on the same leg and an extension on the contralateral side to support stance. Stimulation to support training tasks where the motion of the two feet is in antiphase, such as cycling, could be triggered by a single sensor placed on the crank—EES^{CYCLE}. Leg flexions and contralateral extensions could then be triggered for both sides at appropriate moments during the cycle. A second sensor could be placed on a corresponding device frame to maintain the function of the stimulation at various tilts of the device with respect to the ground.

Participants could alternatively trigger stimulation via dedicated ergonomic clickers designed together with the end users—EES^{CLICK}. A first design facilitated button clicking with a motion of fingers pressing against the palm, which was preferred by one participant with reduced finger function. A large lever arm further allowed use with little remnant force and low precision, which facilitated use during treadmill gait training. A second design was in the form of a clicker that could be fixed on a multitude of rails, such as parallel bars or that of a walker. Training in a hand-assisted tricycle exploited the coupling between upper and lower limbs to trigger amplitude-modulated stimulation. The timing of stimulation and the stimulation amplitudes were determined as a function of the measured angles and forces provided by the upper limbs, recorded by a sensorized pedal (X-Power, SRM GmbH). This enabled the system to proportionally engage the arms and legs in a coordinated manner.

Functional ambulatory categories

Rehabilitation activities in various devices were classified as follows on the basis of the FAC of patients for whom such training would be most relevant: FAC 0, nonfunctional ambulator; FAC 1, ambulator, dependent on physical assistance—level I indicates a patient who requires continuous manual contact to support body weight and to maintain balance or to assist coordination; FAC 2, ambulator, dependent on physical assistance—level II indicates a patient who requires intermittent or continuous light touch to assist balance or coordination; FAC 3, ambulator, dependent on supervision: indicates a patient who can ambulate on level surface without manual contact of another person but requires standby guarding of one person either for safety or verbal cueing; FAC 4, ambulator, independent level surface only—indicates a patient who can ambulate independently on a level surface but requires supervision to negotiate (e.g., stairs, inclines, and nonlevel surfaces); and FAC 5, ambulator, independent—indicates a patient who can walk everywhere independently, including stairs.

Physiological metrics

Electromyographic recordings

Electromyographic (EMG) activity of selected muscles was acquired at a 2000-Hz sample rate using the 16-channel wireless Delsys Trigno sensors (Delsys Inc., Natick, MA, USA) with bipolar surface electrodes placed over the following muscles of the lower limbs: iliopsoas, rectus femoris (RF), vastus lateralis, semitendinosus (ST), tibialis anterior (TA), medial gastrocnemius (MG), and soleus. Skin hairs were shaved, and abrasive gel (NuPrep) was used on the area of interest. In Lokomat, the RF and ST sensors were placed 2 and 3 cm proximally to avoid the thigh cuff. For the TA, minisensors were used with the sensing electrodes placed under the shank cuff and the sensor body electrodes placed below. All sensors besides the TA and MG were placed before the patient was positioned in Lokomat.

Lower limb kinematics

Kinematics were either captured by the NGIMU sensors or using the Delsys sensors already used for EMG acquisition that themselves integrate IMUs that sample at 100 Hz. Given that their positioning was determined by the location of the relevant muscle, it was not always optimal to capture the necessary motion. We therefore placed additional IMUs, Physilog 5 (Gait-Up, Switzerland), on the participants or on the rehabilitation device and recorded acceleration and angular velocity at 100 Hz. These synchronize together via a proprietary radiofrequency protocol, up to 10 units, and have storage capacity of up to 10 hours.

Device data streaming

Lokomat and Myosuit integrated continuous data recording of torques and angles of hip and knee joints, where the devices actively assist. The treadmill speed and BWS of the former was also recorded. The number of successful steps in the C-Mill was collected using video recordings given that the device's own force plate gait detection algorithm did not perform reliably with our patient population, likely because of foot drag and insufficient loading on the treadmill.

Sensorized insoles

Sensorized insoles (Moticon OpenGo, AG, Germany) were used to quantify loading of each foot during training in the Myosuit. Each insole contained 16 pressure cells and an IMU that recorded at 100 Hz. Data were recorded onboard and were retrieved via a mobile app after a recording session. Insoles already inside the participant's shoes were removed before placing the sensorized ones.

Trike sensors

Forces exerted by the arms and legs during use of the trike were recorded using a sensorized X-Power pedal (SRM GmbH, Germany). The electronics and rechargeable batteries were housed inside the spindle, and the waterproof shell protected the electronics of the device to allow outdoor cycling without damaging the device. The pedal integrated a dynamometer, gyroscopes, and accelerometers to measure radial and tangential forces, crank angle, and radial velocity. The radial and tangential components of the force together gave the magnitude and direction of the total force. The tangential force was the applied force provided by the user, whereas the radial force gave information about the inertia.

Data processing and statistics

Analysis of lower limb muscle activity

The electromyographic activity from lower limb muscles was processed according to the SENIAM (Surface Electromyography for the Noninvasive Assessment of Muscles) standards for electromyographic recordings. Displayed electromyographic activities during the various rehabilitation activities were band-pass–filtered between 10 and 450 Hz (fourth-order Butterworth filter). Normalized electromyographic envelopes were generated using a moving average of the rectified electromyographic signal within a centered 250-ms time window. These were used in quantifications to compare conditions with and without stimulation during a rehabilitation exercise by extracting the envelope maximum per activity cycle.

Analysis of lower limb kinetics

The acceleration and angular velocity collected by the Delsys and Physilog 5 sensors were passed through a data-fusion algorithm (*51*) to extract sensor orientation with respect to Earth in quaternion representation. Roll, pitch, and yaw angles were then calculated using one of two representations (*zyx* or *zyz*), depending on the sensor placement with respect to its axis with greatest motion, such that there would be no discontinuities in the pitch.

Statistics

Statistical analysis was performed in R, Prism GraphPad, or MATLAB. Comparisons between two conditions were performed using nonparametric Mann-Whitney rank sum test for unpaired samples or Wilcoxon signed-rank test for paired samples. Comparisons involving more than two categories were performed using nonparametric Kruskal-Wallis tests. P values for each test are reported as follows: $^{*}P < 0.05$, $^{**}P < 0.01$, and $^{***}P < 0.001$.

Rehabilitation devices

Erigo

The Erigo Pro (Hocoma, part of the DIH Medical group) is a motorized tilt table with an integrated robotic stepping device allowing for early and safe mobilization of people with neurological disorders (*52*, *53*). Two harness straps were used to secure the patient's chest and pelvis to the table. The feet were placed onto the individual foot plates that are fixed at the toe but allow the ankle to be lifted. The thighs were strapped into motorized cuffs that drive the active stepping, alternating between hip and knee, flexion and extension. The range of motion of the hip was set by the physiotherapist and remained unchanged throughout the exercise period. Body weight loading can be increased to ensure stabilization of the patient in the upright position. The tilt table can be inclined gradually from horizontal (0°) to vertical (90°). The stepping speed can be set from 0 to 80 steps per minute. An IMU was fixed on the verticalization table to record the exact angle of the table, and two IMUs were placed on the right and left cyclic leg supports to detect cyclic leg movement events. Raw IMU data were streamed to the interactive software application and converted into quaternions to trigger updates of the stimulation.

MOTOmed

The MOTOmed viva2 light (RECK-Technik GmbH & Co. KG, Germany) is a leg trainer, or rehabilitation bicycle, for passive and active training of the upper and lower limbs. Wheelchair-bound patients positioned themselves in front of the device. Each foot was then strapped onto a pedal, and the patient held onto fixed handlebars when the device was active. Pedaling speed can be set from 0 to 60 rpm when in passive mode. The device has a built-in spasm control that stops the pedaling when a sudden torque is detected. This feature was turned off during the present protocol because EES can provoke controlled muscle activity that can be mistaken for spasms. One IMU was placed on a chosen foot crank (right or left), and raw signals were streamed to the interactive software application to control stimulation.

Lokomat

The Lokomat Pro (Hocoma, part of the DIH Medical group, Switzerland) is a robotic treadmill gait trainer that provides therapy under controlled conditions while supporting patients with mild to severe walking impairments. The device is able to bring highly impaired individuals to a walking state by providing them with an adequate level of assistance through the hip and knee actuated joints and the BWS system of the device. The two leg orthoses of the Lokomat were attached to the patient's legs, and they induced flexion and extension movements of the hip and knee joints in the sagittal plane. The movement speed of the orthoses was synchronized with the treadmill speed, which can be adapted. The movement of the patient's ankles was not directly controlled by the orthosis: Only a passive foot lifter was used to avoid foot drag. Joint torques and angles were measured from force sensors and potentiometers integrated in the orthoses. The legs of the patient were moved along a reference trajectory. The robotic assistance was manually adjusted by the therapist to allow more freedom for the patient and to challenge the patient to actively contribute to the walking pattern. The patient was relieved from their body weight through a harness connected to a BWS system that ensured a controllable unloading that could also be adjusted to match the patient's need.

C-Mill

C-Mill (Motek Medical B.V., part of the DIH Medical group, the Netherlands) is a treadmill with parallel bars and integrated BWS. The device was enhanced by augmented reality enabled by a force plate located under the treadmill belt and a beamer projecting visual content on the belt. Real-time algorithms processing the force plate data enabled the projection of interactive games or performance feedback on the treadmill belt. An integrated screen in front of the patient was used for interactive games or visual feedback. All of the data were recorded, and statistics were exported after the session. The C-Mill can be used for balance, steps, and locomotor training.

Rysen

Rysen (Motek Medical B.V., part of the DIH Medical group, the Netherlands) is a dynamic three-dimensional (3D) overground BWS robotic system for gravity assistance and locomotion restoration intended to be safe and power efficient and to assist patients with walking impairments to move freely in a large workspace. Rysen decouples the degrees of freedom between motors to provide slow/high-torque motors for vertical motion and fast/low-torque motors for horizontal motion, supporting patients with personalized vertical and horizontal assistive forces. These conditions enable patients to operate in a large workspace (10.5 m by 2.9 m) while receiving adjustable supportive forces, thus empowering patients to walk over ground with a natural, upright, and hands-free posture.

Myosuit

Myosuit (Myosuit Gamma, MyoSwiss AG, Zurich, Switzerland) is a lightweight wearable robot for the lower limbs. The device was designed to support the user against gravity through active and passive elements aligned with the working direction of the major hip and knee muscles. The active components of Myosuit include a backpack-like compartment containing the motors, battery, and control unit and a knee orthosis per leg, attached to the thigh and shank using Velcro straps. IMUs are integrated into the orthoses to detect gait events and time the assistance of the device. One cable, or "artificial tendon," per leg is routed from the motor in the backpack, across the buttock, over a hinge at the knee, and lastly anchored to the shank. By winding up these tendons, Myosuit supports synergistic extension of the hip and knee joint. Passive elastomer springs, consisting of elastic rubber bands, cross the hips anteriorly and connect the waist strap of the backpack to the thigh interfaces. These passive elements support flexion of the hip and act in an antagonistic manner to the active elements described before. During hip extension and the stance phase of the gait, the springs are extended and store elastic energy, which is eventually returned in the swing phase of walking.

For the purposes of this study, Myosuit was used in two modes: "zero-force" mode and "assistance" mode. In zero-force mode, no active forces were applied to the user, so Myosuit only compensates for the added inertia, stiffness of the passive elements, and friction in the cables. In assistance mode, Myosuit actively supported weight-bearing during the stance phase of walking. Shortly after heel strike (detected by the IMU on each shank) of each leg, the ipsilateral artificial tendon of the robotic device was tensioned by an electric motor at a rate that was modulated by the user's cadence and reached a peak magnitude that was proportional to the momentary knee angle, where higher cadences resulted in higher rates of force application and more knee flexion resulted in a higher magnitude. The tension on the cable was held until the hip angle crossed a threshold that, by default, was set to be 0° (femur parallel to the gravity vector) but could be modulated by the user to shorten or extend the duration of assistance. Upon crossing the said threshold, the artificial tendon was slacked, releasing the leg and seamlessly allowing it to advance forward to the swing phase of the gait cycle until the subsequent heel strike.

Trike

Go-Tryke (GBY Ltd., Switzerland) is a recumbent tricycle specially designed for people with reduced mobility and is suitable for paraplegic and tetraplegic patients. The tricycle incorporates several features that facilitate its use for people with reduced mobility. The tricycle has a built-in electrical motor that compensates for the lack of traction and can be adjusted according to the user's needs. Also, a reverse gear allows for increased handling of the trike and two braking wheels at the front enhance stability. Last, the seat height and the adjustable steering handlebar make it easy to transfer to and from the user's wheelchair. In the case of disabled lower limbs, these are set in motion via the connected dual pedals that enable simultaneous arm and leg motion. The movement of the upper and lower limbs is mechanically coupled. The trike has a contralateral setup between arms and legs, and the movement of the contralateral arm with respect to one leg is synchronized. At any given time and position on the cycle, both are in the same extension or flexion phase. On the basis of this setup, the alternating movement of arms and legs in rhythm is respected and allows the participant to perform a physiological and coordinated movement.

Walker

The Dolomite Soprano Rollator (model D12030, Invacare Dolomite AB, Sweden) is an all-terrain walker with 25-cm wheels and a large wheelbase. The frame is designed to eliminate the rear forks, creating more room for the legs between the back wheels. The brake handles and wedge-shaped hand pad offer a secure and comfortable grip. The cable-less braking system uses stainless-steel rods encased in the frame to actuate the brake. The brake shoe is designed to catch dirt and stones before they reach the brake pads. Height-adjustable handles also rotate for an ideal wrist positioning.

Supplementary Materials

The PDF file includes:

Figs. S1 to S3
Table S1

Other Supplementary Material for this manuscript includes the following:

MDAR Reproducibility Checklist

REFERENCES AND NOTES

1. V. R. Edgerton, G. Courtine, Y. P. Gerasimenko, I. Lavrov, R. M. Ichiyama, A. J. Fong, L. L. Cai, C. K. Otoshi, N. J. K. Tillakaratne, J. W. Burdick, R. R. Roy, Training locomotor networks. *Brain Res. Rev.* **57**, 241–254 (2008).
2. V. Dietz, K. Fouad, Restoration of sensorimotor functions after spinal cord injury. *Brain* **137**, 654–667 (2014).
3. V. Dietz, S. J. Harkema, Locomotor activity in spinal cord-injured persons. *J. Appl. Physiol.* **96**, 1954–1960 (2004).
4. C. Kathe, M. A. Skinnider, T. H. Hutson, N. Regazzi, M. Gautier, R. Demesmaeker, S. Komi, S. Ceto, N. D. James, N. Cho, L. Baud, K. Galan, K. J. E. Matson, A. Rowald, K. Kim, R. Wang, K. Minassian, J. O. Prior, L. Asboth, Q. Barraud, S. P. Lacour, A. J. Levine, F. Wagner, J. Bloch, J. W. Squair, G. Courtine, The neurons that restore walking after paralysis. *Nature* **611**, 540–547 (2022).
5. M. A. Anderson, J. W. Squair, M. Gautier, T. H. Hutson, C. Kathe, Q. Barraud, J. Bloch, G. Courtine, Natural and targeted circuit reorganization after spinal cord injury. *Nat. Neurosci.* **25**, 1584–1596 (2022).
6. R. R. Roy, S. J. Harkema, V. R. Edgerton, Basic concepts of activity-based interventions for improved recovery of motor function after spinal cord injury. *Arch. Phys. Med. Rehabil.* **93**, 1487–1497 (2012).
7. E. C. Field-Fote, Exciting recovery: Augmenting practice with stimulation to optimize outcomes after spinal cord injury. *Prog. Brain Res.* **218**, 103–126 (2015).
8. D. Borton, S. Micera, J. d. R. Millán, G. Courtine, Personalized neuroprosthetics. *Sci. Transl. Med.* **5**, 210rv2 (2013).
9. J. L. Emken, R. Benitez, D. J. Reinkensmeyer, Human-robot cooperative movement training: Learning a novel sensory motor transformation during walking with robotic assistance-as-needed. *J. Neuroeng. Rehabil.* **4**, 8 (2007).
10. G. L. Rosa, M. Avola, T. D. Gregorio, R. S. Calabrò, M. P. Onesta, Gait recovery in spinal cord injury: A systematic review with metanalysis involving new rehabilitative technologies. *Brain Sci.* **13**, 703 (2023).
11. G. Stampacchia, V. Gazzotti, M. Olivieri, E. Andrenelli, D. Bonaiuti, R. S. Calabro, S. M. Carmignano, A. Cassio, C. Fundaro, I. Companini, D. Mazzoli, S. Cerulli, C. Chisari, V. Colombo, S. Dalise, D. Mazzoleni, C. Melegari, A. Merlo, P. Boldrini, S. Mazzoleni, F. Posteraro, M. Mazzucchelli, P. Benanti, E. Castelli, F. Draicchio, V. Falabella, S. Galeri,

F. Gimigliano, M. Grigioni, S. Mazzon, F. Molteni, G. Morone, M. Petrarca, A. Picelli, M. Senatore, G. Turchetti, E. Bizzarrini, Gait robot-assisted rehabilitation in persons with spinal cord injury: A scoping review. *NeuroRehabilitation* **51**, 609–647 (2022).
12. L. J. Holanda, P. M. M. Silva, T. C. Amorim, M. O. Lacerda, C. R. Simão, E. Morya, Robotic assisted gait as a tool for rehabilitation of individuals with spinal cord injury: A systematic review. *J. Neuroeng. Rehabil.* **14**, 126 (2017).
13. J.-B. Mignardot, C. G. Le Goff, R. van den Brand, M. Capogrosso, N. Fumeaux, H. Vallery, S. Anil, J. Lanini, I. Fodor, G. Eberle, A. Ijspeert, B. Schurch, A. Curt, S. Carda, J. Bloch, J. von Zitzewitz, G. Courtine, A multidirectional gravity-assist algorithm that enhances locomotor control in patients with stroke or spinal cord injury. *Sci. Transl. Med.* **9**, eaah3621 (2017).
14. H. J. A. van Hedel, G. Severini, A. Scarton, A. O'Brien, T. Reed, D. Gaebler-Spira, T. Egan, A. Meyer-Heim, J. Graser, K. Chua, D. Zutter, R. Schweinfurther, J. Carsten Möller, L. P. Paredes, A. Esquenazi, S. Berweck, S. Schroeder, B. Warken, A. Chan, A. Devers, J. Petioky, N.-J. Paik, W.-S. Kim, P. Bonato, M. Boninger, ARTIC network, Advanced Robotic Therapy Integrated Centers (ARTIC): An international collaboration facilitating the application of rehabilitation technologies. *J. Neuroeng. Rehabil.* **15**, 30 (2018).
15. A. Piira, A. Lannem, M. Sørensen, T. Glott, R. Knutsen, L. Jørgensen, K. Gjesdal, N. Hjeltnes, S. Knutsen, Robot-assisted locomotor training did not improve walking function in patients with chronic incomplete spinal cord injury: A randomized clinical trial. *J. Rehabil. Med.* **51**, 385–389 (2019).
16. S. Mazzoleni, E. Battini, A. Rustici, G. Stampacchia, "An integrated gait rehabilitation training based on functional electrical stimulation cycling and overground robotic exoskeleton in complete spinal cord injury patients: Preliminary results" in *2017 International Conference on Rehabilitation Robotics (ICORR)* (IEEE, 2017), pp. 289–293.
17. A. Schicketmueller, G. Rose, M. Hofmann, Feasibility of a sensor-based gait event detection algorithm for triggering functional electrical stimulation during robot-assisted gait training. *Sensors* **19**, 4804 (2019).
18. A. J. del-Ama, Á. Gil-Agudo, J. L. Pons, J. C. Moreno, Hybrid FES-robot cooperative control of ambulatory gait rehabilitation exoskeleton. *J. Neuroeng. Rehabil.* **11**, 27 (2014).
19. J. Mehrholz, J. Kugler, M. Pohl, Locomotor training for walking after spinal cord injury. *Spine* **33**, E768–E777 (2008).
20. C. Tefertiller, B. Pharo, N. Evans, P. Winchester, Efficacy of rehabilitation robotics for walking training in neurological disorders: A review. *J. Rehabil. Res. Dev.* **48**, 387 (2011).
21. V. R. Edgerton, S. Harkema, Epidural stimulation of the spinal cord in spinal cord injury: Current status and future challenges. *Expert Rev. Neurother.* **11**, 1351–1353 (2011).
22. M. L. Gill, P. J. Grahn, J. S. Calvert, M. B. Linde, I. A. Lavrov, J. A. Strommen, L. A. Beck, D. G. Sayenko, M. G. V. Straaten, D. I. Drubach, D. D. Veith, A. R. Thoreson, C. Lopez, Y. P. Gerasimenko, V. R. Edgerton, K. H. Lee, K. D. Zhao, Neuromodulation of lumbosacral spinal networks enables independent stepping after complete paraplegia. *Nat. Med.* **24**, 1677–1682 (2018).
23. J. S. Calvert, P. J. Grahn, J. A. Strommen, I. A. Lavrov, L. A. Beck, M. L. Gill, M. B. Linde, D. A. Brown, M. G. V. Straaten, D. D. Veith, C. Lopez, D. G. Sayenko, Y. P. Gerasimenko, V. R. Edgerton, K. D. Zhao, K. H. Lee, Electrophysiological guidance of epidural electrode array implantation over the human lumbosacral spinal cord to enable motor function after chronic paralysis. *J. Neurotrauma* **36**, 1451–1460 (2019).
24. E. Formento, K. Minassian, F. Wagner, J. B. Mignardot, C. G. L. Goff-Mignardot, A. Rowald, J. Bloch, S. Micera, M. Capogrosso, G. Courtine, Electrical spinal cord stimulation must preserve proprioception to enable locomotion in humans with spinal cord injury. *Nat. Neurosci.* **21**, 1728–1741 (2018).
25. Y. P. Gerasimenko, I. A. Lavrov, G. Courtine, R. M. Ichiyama, C. J. Dy, H. Zhong, R. R. Roy, V. R. Edgerton, Spinal cord reflexes induced by epidural spinal cord stimulation in normal awake rats. *J. Neurosci. Methods* **157**, 253–263 (2006).
26. F. Rattay, S. Resatz, P. Lutter, K. Minassian, B. Jilge, M. R. Dimitrijevic, Mechanisms of electrical stimulation with neural prostheses. *Neuromodulation* **6**, 42–56 (2003).
27. M. Capogrosso, N. Wenger, S. Raspopovic, P. Musienko, J. Beauparlant, L. B. Luciani, G. Courtine, S. Micera, A computational model for epidural electrical stimulation of spinal sensorimotor circuits. *J. Neurosci.* **33**, 19326–19340 (2013).
28. E. M. Moraud, M. Capogrosso, E. Formento, N. Wenger, J. DiGiovanna, G. Courtine, S. Micera, Mechanisms underlying the neuromodulation of spinal circuits for correcting gait and balance deficits after spinal cord injury. *Neuron* **89**, 814–828 (2016).
29. A. Rowald, S. Komi, R. Demesmaeker, E. Baaklini, S. D. Hernandez-Charpak, E. Paoles, H. Montanaro, A. Cassara, F. Becce, B. Lloyd, T. Newton, J. Ravier, N. Kinany, M. D'Ercole, A. Paley, N. Hankov, C. Varescon, L. McCracken, M. Vat, M. Caban, A. Watrin, C. Jacquet, L. Bole-Feysot, C. Harte, H. Lorach, A. Galvez, M. Tschopp, N. Herrmann, M. Wacker, L. Geernaert, I. Fodor, V. Radevich, K. V. D. Keybus, G. Eberle, E. Pralong, M. Roulet, J.-B. Ledoux, E. Fornari, S. Mandija, L. Mattera, R. Martuzzi, B. Nazarian, S. Benkler, S. Callegari, N. Greiner, B. Fuhrer, M. Froeling, N. Buse, T. Denison, R. Buschman, C. Wende, D. Ganty, J. Bakker, V. Delattre, H. Lambert, K. Minassian, C. A. T. van den Berg, A. Kavounoudias, S. Micera, D. V. D. Ville, Q. Barraud, E. Kurt, N. Kuster, E. Neufeld, M. Capogrosso, L. Asboth, F. B. Wagner, J. Bloch, G. Courtine, Activity-dependent spinal cord neuromodulation rapidly restores trunk and leg motor functions after complete paralysis. *Nat. Med.* **28**, 260–271 (2022).
30. M. K. Holden, K. M. Gill, M. R. Magliozzi, J. Nathan, L. Piehl-Baker, Clinical gait assessment in the neurologically impaired. Reliability and meaningfulness. *Phys. Ther.* **64**, 35–40 (1984).
31. F. B. Wagner, J.-B. Mignardot, C. G. Le Goff-Mignardot, R. Demesmaeker, S. Komi, M. Capogrosso, A. Rowald, I. Seáñez, M. Caban, E. Pirondini, M. Vat, L. A. McCracken, R. Heimgartner, I. Fodor, A. Watrin, P. Seguin, E. Paoles, K. Van Den Keybus, G. Eberle, B. Schurch, E. Pralong, F. Becce, J. Prior, N. Buse, R. Buschman, E. Neufeld, N. Kuster, S. Carda, J. von Zitzewitz, V. Delattre, T. Denison, H. Lambert, K. Minassian, J. Bloch, G. Courtine, Targeted neurotechnology restores walking in humans with spinal cord injury. *Nature* **563**, 65–71 (2018).
32. K. Y. Nam, H. J. Kim, B. S. Kwon, J.-W. Park, H. J. Lee, A. Yoo, Robot-assisted gait training (Lokomat) improves walking function and activity in people with spinal cord injury: A systematic review. *J. Neuroeng. Rehabil.* **14**, 24 (2017).
33. M. Laubacher, C. Perret, K. J. Hunt, Work-rate-guided exercise testing in patients with incomplete spinal cord injury using a robotics-assisted tilt-table. *Disabil. Rehabil. Assist. Technol.* **10**, 433–438 (2014).
34. M. Plooij, U. Keller, B. Sterke, S. Komi, H. Vallery, J. von Zitzewitz, Design of RYSEN: An intrinsically safe and low-power three-dimensional overground body weight support. *IEEE Robot. Autom. Lett.* **3**, 2253–2260 (2018).
35. M. Plooij, S. Apte, U. Keller, P. Baines, B. Sterke, L. Asboth, G. Courtine, J. von Zitzewitz, H. Vallery, Neglected physical human-robot interaction may explain variable outcomes in gait neurorehabilitation research. *Sci. Robot.* **6**, eabf1888 (2021).
36. L.-W. Chou, S. A. Binder-Macleod, The effects of stimulation frequency and fatigue on the force–intensity relationship for human skeletal muscle. *Clin. Neurophysiol.* **118**, 1387–1396 (2007).
37. M. Vromans, P. D. Faghri, Functional electrical stimulation-induced muscular fatigue: Effect of fiber composition and stimulation frequency on rate of fatigue development. *J. Electromyogr. Kinesiol.* **38**, 67–72 (2018).
38. A. S. Gorgey, C. D. Black, C. P. Elder, G. A. Dudley, Effects of electrical stimulation parameters on fatigue in skeletal muscle. *J. Orthop. Sports Phys. Ther.* **39**, 684–692 (2009).
39. F. L. Haufe, K. Schmidt, J. E. Duarte, P. Wolf, R. Riener, M. Xiloyannis, Activity-based training with the Myosuit: A safety and feasibility study across diverse gait disorders. *J. Neuroeng. Rehabil.* **17**, 135 (2020).
40. P. Gad, Y. Gerasimenko, S. Zdunowski, A. Turner, D. Sayenko, D. C. Lu, V. R. Edgerton, Weight bearing over-ground stepping in an exoskeleton with non-invasive spinal cord neuromodulation after motor complete paraplegia. *Front. Neurosci.* **11**, 333 (2017).
41. V. Klamroth-Marganska, J. Blanco, K. Campen, A. Curt, V. Dietz, T. Ettlin, M. Felder, B. Fellinghauer, M. Guidali, A. Kollmar, A. Luft, T. Nef, C. Schuster-Amft, W. Stahel, R. Riener, Three-dimensional, task-specific robot therapy of the arm after stroke: A multicentre, parallel-group randomised trial. *Lancet Neurol.* **13**, 159–166 (2014).
42. L. D. Iaco, J. M. Veerbeek, J. C. F. Ket, G. Kwakkel, Upper limb robots for recovery of motor arm function in patients with stroke. *Neurology* **103**, e209495 (2024).
43. R. Arroyo-Fernández, R. Menchero-Sánchez, D. P. Pozuelo-Carrascosa, H. Romay-Barrero, A. Fernández-Maestra, I. Martínez-Galán, Effectiveness of body weight-supported gait training on gait and balance for motor-incomplete spinal cord injuries: A systematic review with meta-analysis. *J. Clin. Med.* **13**, 1105 (2024).
44. H. Lorach, G. Charvet, J. Bloch, G. Courtine, Brain-spine interfaces to reverse paralysis. *Natl. Sci. Rev.* **9**, nwac009 (2022).
45. J. W. Squair, M. Milano, A. de Coucy, M. Gautier, M. A. Skinnider, N. D. James, N. Cho, A. Lasne, C. Kathe, T. H. Hutson, S. Ceto, L. Baud, K. Galan, V. Aureli, A. Laskaratos, Q. Barraud, T. J. Deming, R. E. Kohman, B. L. Schneider, Z. He, J. Bloch, M. V. Sofroniew, G. Courtine, M. A. Anderson, Recovery of walking after paralysis by regenerating characterized neurons to their natural target region. *Science* **381**, 1338–1345 (2023).
46. C. Moritz, E. C. Field-Fote, C. Tefertiller, I. van Nes, R. Trumbower, S. Kalsi-Ryan, M. Purcell, T. W. J. Janssen, A. Krassioukov, L. R. Morse, K. D. Zhao, J. Guest, R. J. Marino, L. M. Murray, J. M. Wecht, M. Rieger, J. Pradarelli, A. Turner, J. D'Amico, J. W. Squair, G. Courtine, Non-invasive spinal cord electrical stimulation for arm and hand function in chronic tetraplegia: A safety and efficacy trial. *Nat. Med.* **30**, 1276–1283 (2024).
47. M. Pasquini, N. D. James, I. Dewany, F.-V. Coen, N. Cho, S. Lai, S. Anil, J. Carpaneto, Q. Barraud, S. P. Lacour, S. Micera, G. Courtine, Preclinical upper limb neurorobotic platform to assess, rehabilitate, and develop therapies. *Sci. Robot.* **7**, eabk2378 (2022).
48. T. Milekovic, E. M. Moraud, N. Macellari, C. Moerman, F. Raschellà, S. Sun, M. G. Perich, C. Varescon, R. Demesmaeker, A. Bruel, L. N. Bole-Feysot, G. Schiavone, E. Pirondini, C. YunLong, L. Hao, A. Galvez, S. D. Hernandez-Charpak, G. Dumont, J. Ravier, C. G. L. Goff-Mignardot, J.-B. Mignardot, G. Carparelli, C. Harte, N. Hankov, V. Aureli, A. Watrin, H. Lambert, D. Borton, J. Laurens, I. Vollenweider, S. Borgognon, F. Bourre, M. Goillandeau, W. K. D. Ko, L. Petit, Q. Li, R. Buschman, N. Buse, M. Yaroshinsky, J.-B. Ledoux, F. Becce, M. C. Jimenez, J. F. Bally, T. Denison, D. Guehl, A. Ijspeert, M. Capogrosso, J. W. Squair, L. Asboth, P. A. Starr, D. D. Wang, S. P. Lacour, S. Micera, C. Qin,

J. Bloch, E. Bezard, G. Courtine, A spinal cord neuroprosthesis for locomotor deficits due to Parkinson's disease. *Nat. Med.* **29**, 2854–2865 (2023).
49. M. P. Powell, N. Verma, E. Sorensen, E. Carranza, A. Boos, D. P. Fields, S. Roy, S. Ensel, B. Barra, J. Balzer, J. Goldsmith, R. M. Friedlander, G. F. Wittenberg, L. E. Fisher, J. W. Krakauer, P. C. Gerszten, E. Pirondini, D. J. Weber, M. Capogrosso, Epidural stimulation of the cervical spinal cord for post-stroke upper-limb paresis. *Nat. Med.* **29**, 689–699 (2023).
50. R. Rupp, F. Biering-Sørensen, S. P. Burns, D. E. Graves, J. Guest, L. Jones, M. S. Read, G. M. Rodriguez, C. Schuld, K. E. Tansey-MD, K. Walden, S. Kirshblum, International standards for neurological classification of spinal cord injury. *Top. Spinal Cord. Inj. Rehabil.* **27**, 1–22 (2021).
51. S. O. H. Madgwick, A. J. L. Harrison, R. Vaidyanathan, "Estimation of IMU and MARG orientation using a gradient descent algorithm" in *2011 IEEE International Conference on Rehabilitation Robotics* (IEEE, 2011), pp. 1–7.
52. T. Yoshida, K. Masani, D. G. Sayenko, M. Miyatani, J. A. Fisher, M. R. Popovic, Cardiovascular response of individuals with spinal cord injury to dynamic functional electrical stimulation under orthostatic stress. *IEEE Trans. Neural Syst. Rehabil. Eng.* **21**, 37–46 (2013).
53. C. T. D. Craven, H. Gollee, S. Coupaud, M. A. Purcell, D. B. Allan, Investigation of robotic-assisted tilt-table therapy for early-stage spinal cord injury rehabilitation. *J. Rehabil. Res. Dev.* **50**, 367–378 (2013).

Acknowledgments: We would like to thank M. Wacker and I. Fodor for assistance in multiple physiotherapy sessions; N. Chablais for assistance with figure design; L. McCracken, M. Vat, and J.-P. Miroz for support in patient logistics and patient care; M. Keller, P. Rodrigues, U. Costa, L. Lünenburger, and D. Munari for support, assistance, and training on the Hocoma devices; L. Paredes for the introduction to robotic rehabilitation process along the continuum of care at Rehaklinik Zihlschlacht; and A.-R. Warter-Jouve, L. Dratva, U. Keller, C. Fritsche, and S. B. Ghorbel for technical support during their time at ONWARD Medical. **Funding:** This work was supported by the Swiss National Science Foundation (NCCR Robotics, 51NF40_185543, subproject 1 ReGait++), Wings for Life, Defitech Foundation, International Foundation for Research in Paraplegia, Riders4Riders, Panacée Foundation, Pictet Group Charitable Foundation, Firmenich Foundation, Eurostars (E! 11834 WALKAGAIN), Medtronic (Research Support Agreement NM-2546), and Personalized Health and Related Technologies (PHRT Project #2022-279).
Author contributions: Supervision of all aspects of the work: J.B., J.V.Z., and G.C. Writing of the manuscript: G.C., M.C., N.H., and L.A. Editing of the manuscript: All authors. Conducting sessions: N.H., M.C., M.R, C.V., M.R.S., F.H., M.D., H. Lorach, M.X., R.D., and L.A. Conducting physical therapy: A.G., E.B., A.P., M.T., and N.H. Data analysis: N.H., M.C., S.K., M.R., C.B., F.A., F.H., G.K., M.X., and R.D. Student supervision: J.V.Z., M.C., N.H., M.R.S., S.M., F.W., S.T., R.D., and L.A. Hardware/software development: T.D., N.B., R.B., C.H., R.D., S.K., F.W., M.C., and N.H. Regulatory affair management: M.D., C.J., A.W., H. Lambert, R.D., and L.A. Illustration preparation: N.H., L.A., J.R., and F.M. Funding acquisition: G.C., J.B., J.V.Z., and F.W. Team management: A.W., D.D.B., G.E., H. Lambert, R.R., M.X., A.I., F.W., S.T., J.V.Z., R.D., and L.A. **Competing interests:** G.C., J.B., R.D., J.V.Z., M.C., F.W., S.T., S.K., and L.A. hold various patents in relation to electrical spinal cord stimulation. G.C., J.B., J.V.Z. and H. Lambert are cofounders and shareholders of ONWARD Medical, a company that develops treatments for people with SCI with relationships with the presented work. The other authors declare that they have no competing interests. **Data and materials availability:** Data that support the findings are available in the following data depository: 10.5281/zenodo.12533019. Source data are provided with this paper. Custom-built software and control algorithms will be made available upon reasonable request to gregoire.courtine@epfl.ch.

Submitted 19 December 2023
Accepted 11 February 2025
Published 12 March 2025
10.1126/scirobotics.adn5564

Science Robotics

Augmenting rehabilitation robotics with spinal cord neuromodulation: A proof of concept

Nicolas Hankov, Miroslav Caban, Robin Demesmaeker, Margaux Roulet, Salif Komi, Michele Xiloyannis, Anne Gehrig, Camille Varescon, Martina Rebeka Spiess, Serena Maggioni, Chiara Basla, Gleb Koginov, Florian Haufe, Marina D'Ercole, Cathal Harte, Sergio D. Hernandez-Charpak, Aurelie Paley, Manon Tschopp, Natacha Herrmann, Nadine Intering, Edeny Baaklini, Francesco Acquati, Charlotte Jacquet, Anne Watrin, Jimmy Ravier, Frédéric Merlos, Grégoire Eberlé, Katrien Van den Keybus, Hendrik Lambert, Henri Lorach, Rik Buschman, Nicholas Buse, Timothy Denison, Dino De Bon, Jaime E. Duarte, Robert Riener, Auke Ijspeert, Fabien Wagner, Sebastian Tobler, Léonie Asboth, Joachim von Zitzewitz, Jocelyne Bloch, and Grégoire Courtine

Sci. Robot. **10** (100), eadn5564. DOI: 10.1126/scirobotics.adn5564

Science Robotics (ISSN 2470-9476) is published by the American Association for the Advancement of Science. 1200 New York Avenue NW, Washington, DC 20005. The title *Science Robotics* is a registered trademark of AAAS.